

Morb
University of Basel

Eric Ulrich

June 18, 2019

Contents

1 Abstract	4
2 Introduction	5
2.1 Emergence of antibiotic resistance	5
2.2 β -lactams and resistance against this class of antibiotics	6
2.2.1 β -lactams	8
2.2.2 Resistance of ESBL <i>E. coli</i> against β -lactams	8
2.2.3 General resistance mechanisms	9
2.2.4 ESBL <i>E. coli</i>	10
2.3 Identifying mutations deciding over resistance or susceptibility of ESBL <i>E. coli</i>	10
2.3.1 Principles of the morbidostat	10
2.3.2 Previous morbidostat experiments and expected outcome	11
2.3.3 Illumina and Nanopore sequencing	11
2.4 Aim of this thesis	12
3 Materials and methods	13
3.1 Identifying mutations in ESBL <i>E. coli</i> sample series	13
3.1.1 Pipeline for identifying mutations	14
3.2 ESBL <i>E. coli</i> sampling at the University Hospital of Basel	16
3.2.1 Selection of samples suitable for our analysis	16
3.2.2 Phylogenetic analysis	16
3.3 Assembling and handling procedure of the morbidostat	18
3.3.1 Hardware and setup	18
3.3.2 Morbidostat modes and control	21
3.3.3 Hardware calibration	24
3.4 Safety aspects of morbidostat experiments	24
3.4.1 Gibson cloning	25
3.5 Experimental procedure for culturing with the continuous mode	25
3.5.1 MIC determination	25
3.5.2 Testing the feedback from the continuous culture mode	26
3.5.3 Culturing K12 carrying ESBL plasmids with the morbidostat .	26
4 Results	28
4.1 Analyzing ESBL <i>E. coli</i> isolates from patients of the University hospital Basel	28
4.1.1 Sample selection	28
4.1.2 Sequencing and assembling	29
4.1.3 SNPs	29

4.1.4	Comparing ESBL genes in the resistant samples and the susceptible samples	33
4.2	Morbidostat experiments	35
4.2.1	Testing the continuous experiment	35
4.2.2	Morbidostat experiment 01	38
4.2.3	Morbidostat experiment 02	38
5	Discussion	39
5.1	Analysis of the ESBL E. coli patient isolates	39
5.1.1	SNPs	39
6	Supplementary	40
6.1	Manual for starting experiments with morbidostat	40
6.2	SNPs with no annotation	40
7	Declaration	43
8	References	44
9	Acknowledgements	50

Chapter 1

Abstract

asdfsdaf

Chapter 2

Introduction

The discovery of penicillin shortly before the Second World War revolutionized human medicine by saving the lives of millions of soldiers and civilians suffering under bacterial infections [11]. Because bacterial infections could now be treated major advances in surgery were possible [45]. Since then antibiotics play a very important role in the health care system and we are heavily depending on those drugs.

Because of the positive effects of penicillin it quickly started to be used in excess and irresponsible. This led to the emergence of penicillin resistance within 32 years after its discovery [45]. Ever since then it was necessary to repetitively introduce new antibiotics to the market because bacteria evolved resistance against previously developed drugs.

2.1 Emergence of antibiotic resistance

Worldwide an emergence of antibiotic resistance is occurring [46]. An increase of antibiotic usage and a decrease of development of new antibiotics are the the main reasons for this emergence [46]. As shown in Figure 2.1 A and B consumption mainly increased for countries where a huge population is associated with middle and lower income [24]. In those two groups the increase between 2000 and 2015 behaved exponentially. Countries where the average income is high show a pretty stable consumption over the recorded years. But the overall consumption is much higher compared to the other groups with middle and low income. This also shows that there is an uneven access to antibiotics.

The development of new antibiotics on the other hand decreased in the last four decades as visible in Figure 2.1 C. When between 1980 and 1984 19 antibiotics were approved by the Food and drug Administration (FDA), only six novel drugs where approved between 2010 and 2014. The decrease of development of new antibiotics mainly has economical reasons. Newly approved antibiotics are usually held in reserve and only prescribed for infections that more established antibiotics can't treat. This heavily limits the investment in return [18]. Additionally antibiotics are only used for a short time. Compared to drugs used for treating chronic diseases this makes antibiotics a lot less profitable [18]. With an estimated cost of 0.5 billion USD development of antibiotics is also very expensive [30]

Antibiotic consumption takes place in two fields. One being the health sector and one being the food industry. Unfortunately in the health sector many antibiotics are prescribed unnecessarily. It was shown that 47 millions prescriptions of antibiotics

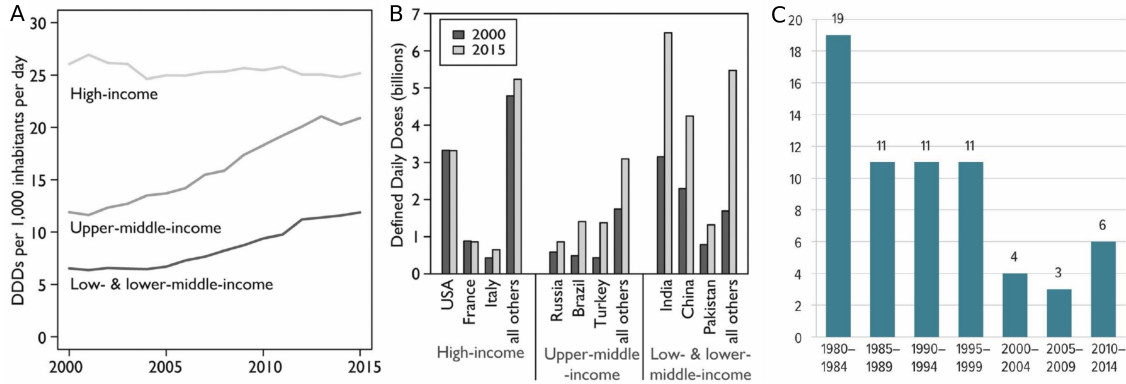


Figure 2.1: A: Consumption of defined daily antibiotic doses per 1000 inhabitants per day over 15 years. B: Antibiotic consumption for selected countries associated with certain incomes. Especially India and other countries with a huge population with a lower income show a tremendous increase of antibiotic consumption [24]. C: Decrease of FDA approved drugs between 1980 and 2014.

in the USA were not needed [3]. Most of them were prescribed for respiratory conditions most commonly caused by viruses [3]. In the food industry it is assumed that in the early 2000s 25-50% of all antibiotic consumption took place [34]. What makes this extremely high usage questionable is that they are mainly used for prophylaxis and to stimulate growth but not to cure animals with diseases.

The combination of increased usage and decreased development brought up resistance of all major bacterial pathogens. In Figure 2.2 the most common resistant pathogens in Swiss hospitals are shown. *Staphylococci aurei*, *streptococci pneumoniae*, *sinterococcus faecalis* and *enterococcus faecilum* which are resistant against different classes of antibiotics decreased in their frequency. This is either because a vaccine was introduced (PCV7 vaccine against several *pneumococcal* strains) or screening of the pathogens was improved. Resistant *escherichia coli* (*E. coli*) are gaining commonness where mainly resistance against the antibiotics fluoroquinolones and extended spectrum β -lactams occurs.

With this thesis I want to focus on extend spectrum β -lactamase (ESBL) *E. coli*. This pathogen evolved resistance against most cephalosporins which are antibiotics belonging to the class of β -lactams.

2.2 β -lactams and resistance against this class of antibiotics

During the 20th century different classes of antibiotics were developed. All of them harm the bacterial pathogen without harming the host because they target specific bacterial metabolic processes. In Figure 2.3 the most common classes of antibiotics (black) and their targets (red) are shown. β -lactams are by far the most commonly prescribed class of antibiotics.

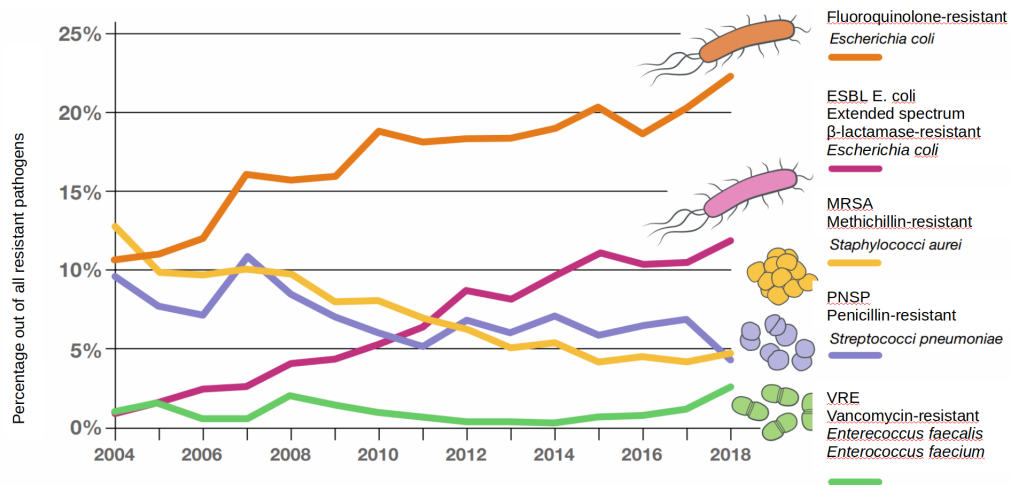


Figure 2.2: Development of resistant pathogens in Swiss hospitals. [4]

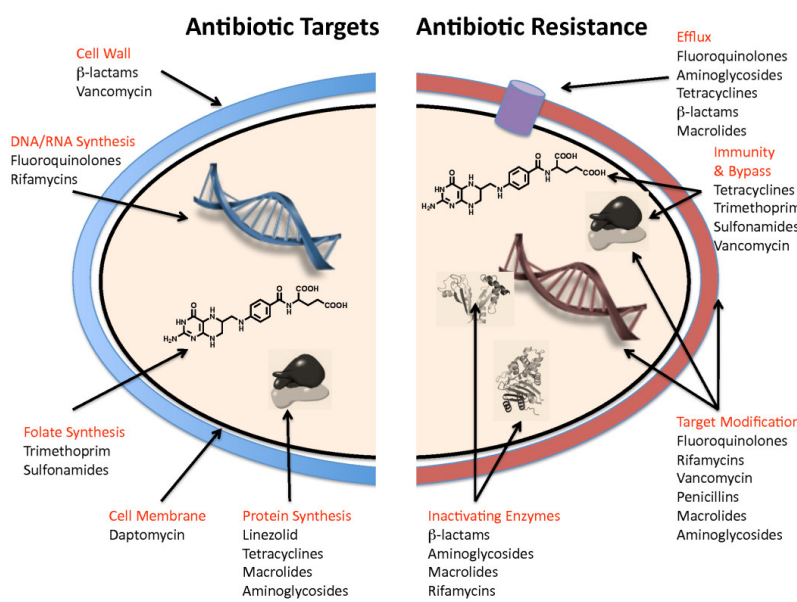


Figure 2.3: Most popular classes of antibiotics and their targets in the bacterial cell [48]

2.2.1 β -lactams

Mechanism of action

β -lactam antibiotics act by inhibiting the synthesis of the peptidoglycan layer of the bacterial cell wall [7]. A damaged cell wall leads to bursting of the cell caused by osmotic pressure. Gram-positive bacteria are especially vulnerable to β -lactams because the peptidoglycan forms the very outer layer of their cell membrane [21]. Peptidoglycan synthesis is inhibited because β -lactams are analogues of the amino acid D-alanyl-D-alanine [20]. Those two amino acids form the terminal residues of the peptide which is attached to N-acetylmuramic acid (NAM). NAM itself is linked repetitively with N-acetylglucosamine (NAG) [20]. The peptide residues of the poly-NAM-NAG chains can be crosslinked by DD-transpeptidases. This cross-linkage results in a mesh-like layer the peptidoglycan [20]. β -lactams bind to the active site of DD-transpeptidases and inhibit their activity irreversibly [20].

Cephalosporins

The β -lactams contain a highly strained and reactive cyclic amide. Five groups of β -lactams exist. Those being penams, penems, carbapenems, monobactams and the cefems [8]. Cephalosporins belonging to the cephems are very important because they showed to be very potent and well tolerated by patients thus they are widely used antibiotics [15]. Cephalosporins are divided into five generations.

First-generation cephalosporins are very active against gram-positive cocci but are not very potent against gram-negative bacteria [19]. **The second generation of cephalosporins** are all active against bacteria covered by first-generation drugs, but have extended coverage against gram-negative bacteria [19]. The tendency of enhanced activity against gram-negative bacteria is further visible in **third-generation cephalosporins**. A common representative of this generation is cefazidime [25]. The Second and third generation of cephalosporins are also known as extended cephalosporins. Only two beta-lactams are classified under the **fourth-generation of cephalosporins**, those being ceftazidime and cefpirome [19]. The newest **fifth generation of cephalosporins** were explicitly developed to target resistant strains of bacteria but unfortunately drugs belonging to this generation are ineffective against enterococci bacteria [19].

2.2.2 Resistance of ESBL *E. coli* against β -lactams

It is assumed that ESBL *E. coli* gained resistance by expressing enzymes called β -lactamases which are able to hydrolyze β -lactams [20]. β -lactamases are able to hydrolyze the cyclic amid of β -lactams [9]. Hydrolyzed β -lactam is no longer able to inhibit the DD-transpeptidase [9].

β -lactamases

Mainly plasmid-mediated β -lactamases are important for resistance because they can be transmitted via horizontal gene-transfer [32]. The first plasmid-mediated β -lactamase in gram-negative bacteria was described in the early 1960s and called β -lactamase TEM-1 [19]. TEM-1 was found worldwide only few years later after

its first isolation [19]. TEM-1 was able to cause resistance against β -lactams of this time. That is why extended cephalosporins such as ceftazidime were developed which couldn't be hydrolyzed by TEM-1 [19].

Another anciently known β -lactamase is called SHV-1 which was isolated for the first time in 1974 [27]. It is encoded chromosomally in the majority of isolates of *K. pneumoniae* but is also plasmid mediated when present in *E. coli* [27].

β -lactamases which are able to hydrolyze extended-spectrum cephalosporins are called extended-spectrum β -lactamases or ESBLs. This resulted in the name ESBL *E. coli* for *E. coli* expressing such β -lactamases.

ESBLs

Next to the TEM and SHV families new β -lactamases were isolated over. One of them is called CTX-M-1 β -lactamase which was clinically isolated for the first time in Germany in 1986 [10]. Because it only has a sequence identity of 40 % compared to TEM or SHV [10] it was categorized as a new β -lactamase family. Later on many variants were isolated and the CTX protein family was subdivided into five subgroups, with CTX-M-1 being one of them [19]. It is assumed that they evolved from the β -lactamase precursor AmpC from *Klyzvera ascorbata* [10]. Even though the first CTX-M-1 was isolated in Germany, it is mostly popular in eastern Europe, South America and Japan [10].

Another β -lactamase family belonging to the ESBLs is called OXA. The OXA family was originally created as a phenotypic rather than a genotypic group, based on a specific hydrolysis profile [10]. Its name comes from the ability to efficiently hydrolyze oxacillin [10].

Originally susceptible to extended cephalosporins, some TEM-1 variants also evolved resistance against extended cephaloporins.

2.2.3 General resistance mechanisms

Generally there are three different strategies for a bacterial cell to reduce susceptibility against antibiotics. One strategy is to make it more difficult for the antibiotic to enter the cell which is effective because many antibiotics have target sites within the cell [6]. The second strategy is to reduce the affinity or to protect the target site of the antibiotic. The last strategy is to reduce the amount of antibiotic molecules which are already within the cell. This is possible by degradation of the compound which we have seen with β -lactamases or by active transport out of the cell.

Some compounds such as β -lactams rely on channels in the membrane of the bacteria called porins in order to reach their target site within the cell. That is because e.g. β -lactams are hydrosphylic and therefore can not just pass the lipophylic membrane by diffusion [32]. Because antibiotics have very specific target sites another mechanism to gain resistance is to change the structure of the target [32]. Some pathogens also protect their target sites by dislodging the compound by increasing the dissociation constant [14]. Active transport of antibiotics out of the cell is possible because bacterial cells are able to express substrate specific efflux pumps. Following this pathway is a widely spread mechanism against most classes of antibiotics [32].

2.2.4 ESBL *E. coli*

In order to minimize unnecessary prescriptions of last resort antibiotics EUCAST publishes breakpoints for every antibiotic. Those breakpoints advice clinicians after which minimal inhibitory concentration (MIC) a pathogen is seen as resistant. They also publish guidelines which should help in choosing the appropriate antibiotic. Interestingly presence of ESBL genes does not guarantee resistance against extended cephalosporins. This means that some ESBL *E. coli* have MICs below the breakpoint published by the EUCAST [43]. It is very important that in such cases cephalosporins are prescribed instead of carbapenems or other last resort antibiotics which are used to treat resistant ESBL *E. coli*.

In the past when ESBL genes were detected by molecular screening the EUCAST recommended to prescribe last resort antibiotics no matter if MIC determination showed cephalosporin susceptibility [28]. By now the EUCAST changed their guidelines and only susceptibility testing determines which antibiotic is chosen for treatment [28]. Unfortunately MIC determination takes about 48 hours which is too long in some cases forcing prescription of carbapenems even though it is unknown if it is actually necessary.

It is not known what the genotypic difference is between ESBL *E. coli* which are susceptible or resistant against cephalosporins.

2.3 Identifying mutations deciding over resistance or susceptibility of ESBL *E. coli*

ESBL genes alone do not determine, whether ESBL *E. coli* are resistant to cephalosporins or not. Instead it is possible that mutations, which have not been identified yet, play an important role in resistance to cephalosporins. Those mutations could be involved in other resistance mechanisms than β -lactam hydrolysis.

Such mutations can be identified by analyzing genomic data of susceptible ESBL *E. coli* which gained resistance by evolution. To get access to such genomic data, ESBL *E. coli* which evolved in a natural environment can be sequenced. It is also possible to analyze genomic data obtained from ESBL *E. coli* which were forced to evolve resistance in vitro. Forcing evolution of resistance in vitro is possible with a device called morbidostat.

2.3.1 Principles of the morbidostat

The morbidostat, originally invented by Toprak *et al.*, is an automated culture device [44]. It allows to force bacteria to gain resistance by applying a constantly high antibiotic pressure. With the morbidostat bacteria are grown in a fixed culture volume in vials. The growth in every vial is constantly monitored. Depending on how fast the bacteria grow an appropriate dose of antibiotics is injected into the vials. Culturing multiple days leads to evolution of resistance as phenotypes with increased resistance are constantly selected.

Several tasks are grouped in cycles and repetitively executed by the morbidostat. Over the defined cycle time the optical densities (ODs) are constantly measured which is represented with red dots in Figure 2.4. At the end of the cycle a fit is calculated approximating all the OD measurements from one cycle which is shown

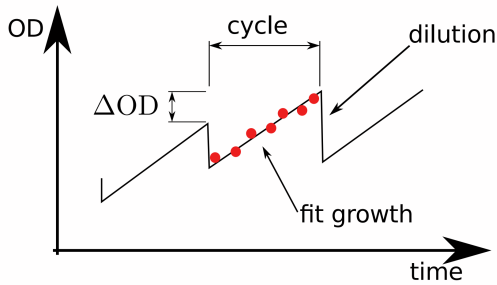


Figure 2.4:

in Figure 2.4 as a black line going through the red dots . From that fit the growth rate is calculated. Also considering the growth of previous cycles, a feedback algorithm decides if and how much drug is injected in which vial. The calculated antibiotic concentration is injected with computer-controllable pumps. If liquids are injected, this also means that the cultures are diluted which is visible in the first OD measurement of the next cycle. As a last step of a cycle, volume which exceeds the culture volume is removed.

2.3.2 Previous morbidostat experiments and expected outcome

Dösselmann *et al.* rebuilt the system in 2015 [17] and used it for colistin resistance. Dösselmann *et al* used the morbidostat in order to study colistin resistance [17]. With the morbidostat they were able to increase the MIC of colistin for *Pseudomonas aeruginosa* 100-fold within 20 days [17]. They identified a mutation pattern associated with colisitn resistance. The mechanism of action for colistin is to displace cations from the phosphate groups of membrane lipids. This leads to disruption of the outer cell membrane causing cell death [13]. Therefore, it is not surprise that Dösselmann *et al* could identify several mutations coding fro proteins involved in the lipopolysaccharide synthesis [17].

2.3.3 Illumina and Nanopore sequencing

Following evolution by studying genomic data relies on accurate sequencing data. Illumina sequencing is a method which produces short reads which are typically 150 base pairs (bp) long. The strong-suit of Illumina sequecning is the low error rate which was dertermined as 0.24 % per base [35]. A common used Illumina sequencing system is the MiSeq-System which is also used for this project. Because the reads are only 150 bases long it is computationally not possible to assemble structurally correct whole-genomes. Oxford Nanopore Technologies produces very long reads which are up to several 100 kbp long. In contrast to Illumina sequencing the error rate per base is 13.6 % [37] which is a lot higher. But because the reads are so long it is possible to assemble structurally correct whole-genomes.

By sequencing on both platforms it is possible to combine the benefits of the long reads of Nanopore with the low error rate of Illumina. This results in very accurate whole genome assemblies.

2.4 Aim of this thesis

The aim of this master thesis is to investigate the resistance evolution of ESBL *E. coli* against the fourth-generation cephalosporin cefepime. The focus is on identifying mutations which accumulated in the genome of resistant ESBL *E. coli* by evolutionary pathways. One part of achieving this aim relies on studying genomic data obtained from ESBL *E. coli* samples taken from patients showing a change in their susceptibility against cefepime. The other part involves assembling a morbidostat and use it to force susceptible ESBL *E. coli* to gain resistance. Similar to the first part, the aim is to follow the evolution of resistance by studying genomic data. The work involves

- DNA sequencing with Oxford Nanopore Technologies
- De novo assembling of ESBL *E. coli* combining Illumina and Nanopore Technology sequencing data
- Development of a bioinformatic analysis pipeline to identify mutations accumulated over time by evolutionary pathways
- Identification of mutations in resistant ESBL *E. coli* patient isolates
- Assembling and troubleshooting of the morbidostat, use it to force ESBL *E. coli* to evolve resistance
- Identification of mutations in resistant ESBL *E. coli* where resistance evolution was forced with the morbidostat
- Providing annotation of the mutations

Chapter 3

Materials and methods

3.1 Identifying mutations in ESBL *E. coli* accumulated by evolving resistance against cefepim

We established a pipeline which allowed us to identify mutations which accumulated by evolutionary pathways while an ESBL *E. coli* strain changed their phenotype from susceptible to cefepime to resistant. This pipeline was based on sequencing data coming from multiple samples which were taken along the evolution of resistance. Samples taken along this pathway are also referred as sample series. The steps of the pipeline are shown in Figure 3.1. The first step was to de novo assemble the genome of For identifying mutations in ESBL *E. coli* Per patient we de novo assembled highly accurate genomes of the sample with the lowest cefepim MIC using Oxford Nanopore Technology and Illumina sequencing data. Those assemblies acted as the reference genome for the sample series of a patient. Illumina sequencing data of all samples from a patient were mapped against the according reference genome. This allowed us to identify mutations which are potentially involved in the resistance mechanism.

Nanopore sequencing

The library was prepared with a ligation sequencing kit (LSK-108) followed with the native barcoding expansion kit. This allowed barcoding of every sample and loading all of them on a single flow cell (FLO-MIN106D). As a sequencing device we used the MinION (Oxford Nanopore Technologies).

As a first step each DNA isolate was diluted to a concentration of 1 µg/µl in 50 µL nuclease free water (NFW). For end-repairing the DNA 7 µL NEBnext Ultra II Endrepair/dA-Tailing enzyme mix were added to each sample and incubated at 20°C for 5 min and at 65°C also for 5 min. After this step every sample was cleaned up by adding 60 µl of AMPure XP beads. The beads were incubated with the samples for 5 minutes on a rotor and then removed on a magnetic rack. Every sample was washed with 200 µL 70% ethanol which was repeated once. The ethanol was removed and every sample was suspended in 25 µL NFW. 2.5 µL of each barcode plus 25 µL of Blunt/TA ligase was added to each sample and incubated for 10 minutes. All the samples were pooled and 500 µl of AMPure XP beads were added. After incubating the pooled sample for 5 minutes on the rotor the sample was washed again twice with 70 % ethanol. All the DNA was eluted in 51 µL NFW. The final sample was

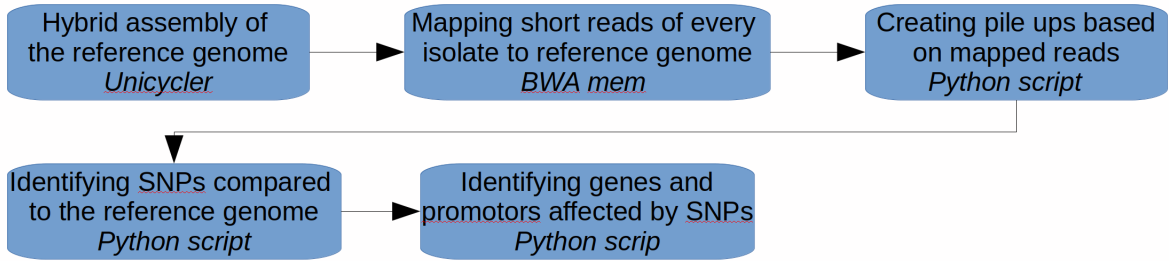


Figure 3.1: Pipe line used for the identification of SNPs and affected genes/promotors

diluted to a concentration of 35 ng/ μ L. Then for adapter ligation 20 μ L BAM, 30 μ L Ultra II ligation master mix and 1 μ L enhancer were added. After 10 minutes of incubation, 40 μ L AMpure XP beads were added and incubated on the rotor for 5 minutes. The supernatant was removed on the magnetic rack and the DNA was washed twice with ABB. The DNA was eluted and incubated for 10 minutes in 15 μ L ELB. Finally the library was prepared by mixing 15 μ L of eluted DNA in ELB with 25.5 μ L LLB and 35 μ L RBF. The resulting library was loaded on the flow cell, which was primed before with a mixture of 480 μ L RBF and 520 μ L of NFW. The sequencing run was started and simultaneously base-called with Albacore.

3.1.1 Pipeline for identifying mutations

We only included patients for our analysis where we ensured that samples coming from the patient were the same ESBL *E. coli* strain. We did that with a phylogenetic analysis for all samples. As a tool for this analysis we used PanX [16].

Identification of mutations

After phylogenetic analysis allowed us to select patients where the collected samples were the same ESBL *E. coli* strain we followed a bioinformatical pipeline in order to identify mutations. The steps of this pilepline are shown in Figure 3.1.

Creating a reference genome

As a first step of the pipeline we built one reference genome per patient based on the sample with the lowest MICs. We did that by combining the Nanopore and the Illumina data of the according sample into a hybrid assembly using Unicycler [47]. Unicycler assembles the short-reads using spades. The long-reads are used for scaffolding.

Annotating the reference genome

Every reference genome was annotated with prokka (v.1.12) [39]. Additionally promotor regions were identified using the promoter prediction tool PePPER [23]. PePPER is a tool which takes whole-genomes as an input and predicts promotor sequences. Those sequences were mapped against the reference genome using

graphmap [42]. Furthermore a promotor data base hosted on EcoCyc was used which contains around 3800 experimentally validated promotors for *E. coli*[40]. The sequences from this database were downloaded and mapped against the reference genome with graphmap aswell [42].

Mapping of short reads

As a next step all the Illumina short-reads from every sample of each patient were mapped against the reference genome with BEW mem and stored as a bam-file [29]. This allowed us to see which base is present in every Illumina read at a certain position of the reference genome.

Creating pile ups

To make easily accessible which base is present in every Illumina read at a certain position we calculated pile-ups. Pile-ups are count matrices which store which base is present how many times at a certain position considering every Illumina read mapped to this position. In order to produce those pile-ups we used a script called pileup.py Because the same reference genome was used for all the samples from one patient all the pile-ups from one patient could be stored in a matrix stack. This allowed us to easily calculate base frequencies, coverage or to identify the most abundant base at a certain position of a sample. The data construction as matrix stack allowed us to easily compare different samples at a position of interest.

Identification of mutations

We identified mutations by comparing the pile-ups of all samples from one patient. In detail a script called analysis_modular.py went through every position of the matrix stack. The most abundant base present in every sample at every position was compared. If the most abundant base varied a SNP was identified. This way were able to find SNPs, deletions and insertions, even though we didn't study the insertions. For the rest of the pipeline only mutations were included where the coverage was at least 30 and the base frequency at least 0.8.

Identification of genes and promotors affected by SNPs

As a last step as seen in Figure 3.1 it was checked if annotation was available for every found mutation. As described in section 3.1.1 genes and promoters were identified for every reference genome.

For checking if a SNP affected a gene, we analyzed the genbank file with biopython [12]. We checked if a mutation was located between a start and an end position of a gene. For checking if a SNP affected a promotor region we analyzed the bam-files which were created with the promoter sequences coming from PePPER and EcoCyc (see 3.1.1). We checked if a SNP was located between a start or end positon of a mapped promotor sequence.

Overlap based whole-genome assembling

For some samples we tried another assembler called canu [26]. Canu is an assembler which assembles the whole-genome based on overlaps of the long-reads. Illumina-

reads can be used to polish errors in the assembly from canu. Polishing is possible with the software called pilon [36].

3.2 ESBL *E. coli* sampling at the University Hospital of Basel

Our collaborators from the clinical microbiology of the University hospital of Basel collected 65 *E. coli* samples of 34 patients. Those collected samples were all screened positive for ESBL genes. This resulted in ESBL *E. coli* sample series with one to four samples per patient. The sampling period was between 2011 and 2015. Sample collection for one patient typically happened within several months.

Screening for ESBL genes

Coming after meeting with Adrian

3.2.1 Selection of samples suitable for our analysis

Our collaborators determined the MICs of every sample for the third-generation cephalosporin ceftazidim and the fourth-generation cephalosporin cefepim. Some sample series showed a significant change of the MICs. Sometimes resistance was gained, but in certain cases resistance was also lost. We were interested in identifying mutations in sample series where susceptibility significantly changed and all the samples from a series were the same ESBL *E. coli* strain.

Determination of the minimal inhibitory concentration

Coming after meeting with Adrian.

3.2.2 Phylogenetic analysis

We checked if a sample series were the same ESBL *E. coli* strain by running a phylogenetic analysis with Illumina sequencing data. For phylogenetic analysis we used a tool called PanX [16]. Illumina data for every sample was provided by our collaborator.

Illumina sequencing

The DNA from the samples was isolated using the EZ1 DNA tissue kit on an EZ1 Advanced XL robotic system (Qiagen). The library for the sequencing was prepared using the Nextera XT library preparation kit (Illumina) and the resulting library was sequenced on a MiSeq Illumina platform [2]. The reads produced with Illumina were trimmed with Trim Galore [5].

PanX

PanX is a tool which clusters samples based on their genes into orthologous clusters. From those clusters, panX identifies the core genome which are genes shared by all

samples in the cluster. Based on those core genomes a strain-level phylogeny can be build, making use of single nucleotide polymorph positions (SNPs) within the core genomes.

PanX used annotated whole-genomes as input files that is why every sample was short-read assembled and annotated. For short-read assembling we used spades (v3.12.0) [33], for annotating the resulting assemblies we used prokka (v.1.12) [39]. Prokka first searches a core set of well characterized protein using BLAST+ and then compares reading frames to a database derived from UniProtKB [38]. The results from prokka were stored in a genbank file for every isolate. Based on those genbank files the PanX analysis was performed.

3.3 Assembling and handling procedure of the morbidostat

The following system is an adapted version of Topraks built differing mainly in its pump system, controlling unit and software. Hardware which was not commercially available was built by the in-house mechanic and electronic workshop.

3.3.1 Hardware and setup

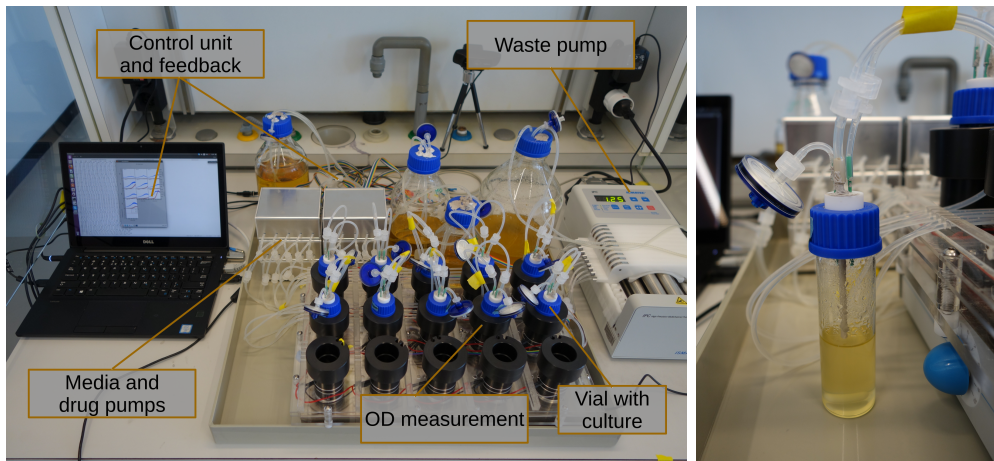


Figure 3.2: Left: Overview of the morbidostat setup. The microcontroller is located behind the drug and media pumps. Right: One vial with all the inlets.

Figure 3.2 shows the morbidostat setup. As a base for our built we used a magnetic stirrer with 15 slots. On that stirrer we placed three layers of acrylic glass which acted as our vial holders. Between the acrylic glass layers the OD measuring units were installed. To block out as much light as possible, the vials were surrounded with black plastic rings as visible in Figure 3.2. The vials placed in the vial holders had three inlets. One inlet was used to inject media or antibiotics, through another one exceeding volume was removed and the last one was used to mount an air filter for pressure equilibration. Even though only one tube per vial was used for injecting fluids each vial was connected to three injecting pumps. Every pump was connected to a bottle with media, a low-concentrated and a high-concentrated antibiotic solution. The tubing from the three pumps per vial was connected to one and led to the vial. Injection of the desired concentration was possible by turning on pumps for certain times. In order to control the pumps and to measure the ODs we used a microcontroller. We connected the microcontroller serially to a PC. The programs on the PC were responsible for initializing morbidostat hardware commands and to store injected antibiotic concentrations as well as measured ODs. This allowed us to see approximately how much resistance was already gained at any time-point of the experiment.

For assembling and testing the hardware we built the morbidostat in the open as shown in Figure 3.2. For the actual experiments we placed the morbidostat insite an hypoxi-station in a bio safety lab 2. This allowed us to culture the bacteria at 37 °C but also to increase the safety.

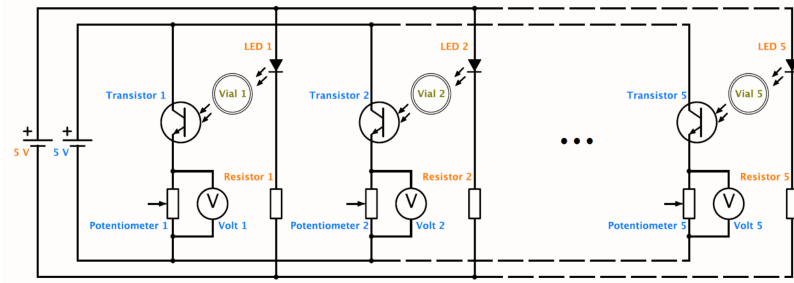


Figure 3.3: Circuit diagram of parallel-connected LED (orange) and phototransistors (blue). This circuit is done independently three times for five vials each. The detector and the LED are orientated in a 135 °angle since this is the best angle for detecting light scattering.

Measuring of optical densities

For measuring the OD a combination of a light emitting diode (LED) and a phototransistor was chosen. We chose OPB608A as a LED with a peak wavelength of 890 nm and PT 333-3C as a phototransistor, both from TT electronics. We made use of the fact that cells cause scattering of a ray of light. For each vial we placed a LED and a phototransistor at the glass wall of the vials orientated in a 135 ° angle towards each other. The LED was constantly on shining light through the cultures. When an OD measurement was initialized by the microcontroller the scattering of the light beam was measured with the phototransistor. LEDs and phototransistors were both connected to independent 5 V circuits. Additionally the OD measuring units were grouped in three groups with five vials corresponding to one row of vials. This means that every row of vials had an independent LED and phototransistor circuit. The circuits of one row of the morbidostat are illustrated in Figure 3.3, where the LED circuit is shown orange and the phototransistor circuit in blue. We connected the five LEDs in parallel and placed a $x \Omega$ resistor after the LEDs. The circuit of the phototransistor was also built in parallel. Each phototransistor had a potentiometer connected in serial, over this potentiometer the voltage was measured. Measuring the scattering worked as follows. Light reaching the phototransistor caused an opening in the semiconductor from the phototransistor which led to an amplification of the current by the transistor. This current reached the potentiometer over which we measured the voltage. The opening of the semiconductor was proportional to the light which reached it. More cells in the suspension caused more scattering, meaning a bigger opening in the semiconductor. A bigger opening led to more current. If more current reached the resistor, the measured voltage was smaller. This means that the measured voltage was proportional to how many cells were in the suspension. By calibration we could translate the voltage to an OD. In order to do so we measured different OD standards with a known OD and stored the corresponding voltages. Measuring multiple OD standards allowed us to calculate a linear equation. This equation was used to convert the voltages to ODs. We chose a potentiometer in order that we can change the sensitivity by changing the resistance over which we measured the voltages. It turned out that the system was not as sensitive as thought in advance, so all the potentiometers were opened as much as possible meaning that the highest possible resistance was chosen.

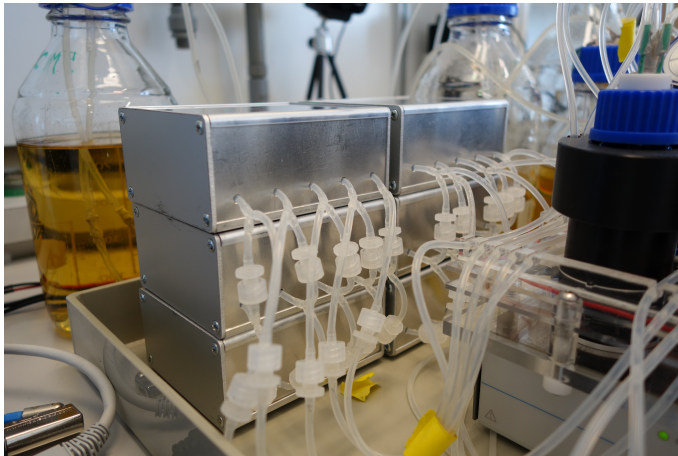


Figure 3.4: Figure left: Vial setup. Figure right: One row of five pumps represents one row of five vials. Since every vial is connected to three pumps, three rows of pumps are stacked on top of each other and connected column by column. This means that one column of three pumps is responsible for injection fluid into one vial. Every outlet from a pump from one column is connected, in order that there is just one tube going to one vial.

Pumps and tubing

Three connected injecting pumps per vial led to 45 injecting pumps in total. Mp6 pumps from microComponents were chosen because they have a compact built, having the size of half an USB stick. This is an improvement because the pumps used by Toprak et al [44] and Doesselmann [17] were peristaltic pumps which were cubic with a size of approximately 4x4x4 cm.

The functional principle is based on a piezoelectric diaphragm in combination with passive check valves which is shown in figure 3.5. By applying voltage a piezo ceramic mounted on a membrane is deformed resulting in a down stroke. When the voltage decreases again the piezo deform again causing an upstroke of the membrane [31]. Because the pump process depends on excitement and relaxation caused by the power, the flow rate generated by the pumps is dependent from the frequency. This also implements that the flow rate is very constant given that the power frequency is also constant. That being the case, the mixing of drug concentration was done by turning on the pumps for a calculated time.

In order to excite and relax the piezo ceramic 230 Volts and a very steady power frequency were needed for this process, making it necessary to control every single pump with a specific mp6-OEM controller. This controller took an input power of 5 V and used about 30 mA of current. The Arduino was not capable of supplying this amount of current for every pump, therefor a separate power adapter was installed to supply the pumps.

The pumps could be controlled by connecting one pin of the controller from the pump to a digital pin of the Arduino. If the pin from the controller was put to ground, the pumps were turned on, if the pin was connected to 5 V the pumps were off. Turning on/off the controller only worked well, when the change of power was very sudden. By adding a pull-down resistor between the digital pins and the ground from the Arduino we could avoid that there was always a very small current flowing through the digital pins. Furthermore it was decided to work with a serial connected

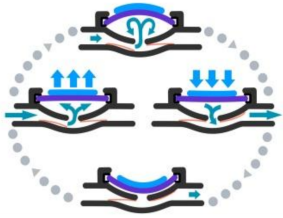


Figure 3.5: Principle of the mp6 pump but two of those piezoelectronics are connected in serial for this pump model [31]

inverter, implementing that when the digital pin was set to low, the inverter caused a power of 5 V which meant that the pumps were off. On the other hand when the digital pin was set to high, the inverter produced a power of 0 V which turned the pumps on. As a waste pump a 16-channel peristaltic pump was used which was directly controlled with a digital pin from the Arduino.

3.3.2 Morbidostat modes and control

One mode was growth_rates which we used in order to record growth rates, in this mode nothing was injected into the vials. Another mode which we called fixed_OD kept the cultures at a desired OD by diluting the culutres with the right amount of media. The last mode was called continuous mode and is the mode that we used to force bacteria to gain resistance. To each vial a different mode could be assigned. We implemented three different modes for culturing bacteria with the morbidostat. CONTINUOUS_MORBIDOSTAT (C) allows to automatically culture bacteria while constantly inhibiting growth with antibiotics. GRWOTH_RATE_EXPERIMENT (G) simply recorded and stored the growth rates of growing bacteria without adding any fluid. FIXED_OD_EXPERIMENT (OD) lept diluting the cultures only with media in a way that the cultures stayed at a fixed OD. Within the same experiments different modes could be used for different vials. A detailed manual for how to start morbidostat experiments from the command line is available in the Section 6.1. The following paragraphs describe the scripts and command chains which controlled the hardware.

Hardware control and data management

The control of the morbidostat was divided into two python scripts running on the laptop and one .ino script running on the microcontroller. Every script is available on GitHub. On the laptop all the scripts are located at `/home/morbidostat/python_morbidostat/python_src/`. Communication of the latop on the microcontroller was possbile via an USB cable enabling serial communication. The two python scripts were `arduino_interface.py` and `morbidostat_experiment.py`. The `arduino_interface.py` was responsible for transmitting commands to the microcontroller via the the serial connection but also for receiving data from the microcontroller. The `morbidostat_experiment.py` script on the other hand was responsible for saving data, initializing cycles and calling different functions depending which mode was chosen. The `arduino_morbidostat.ino` code interpreted and executed the

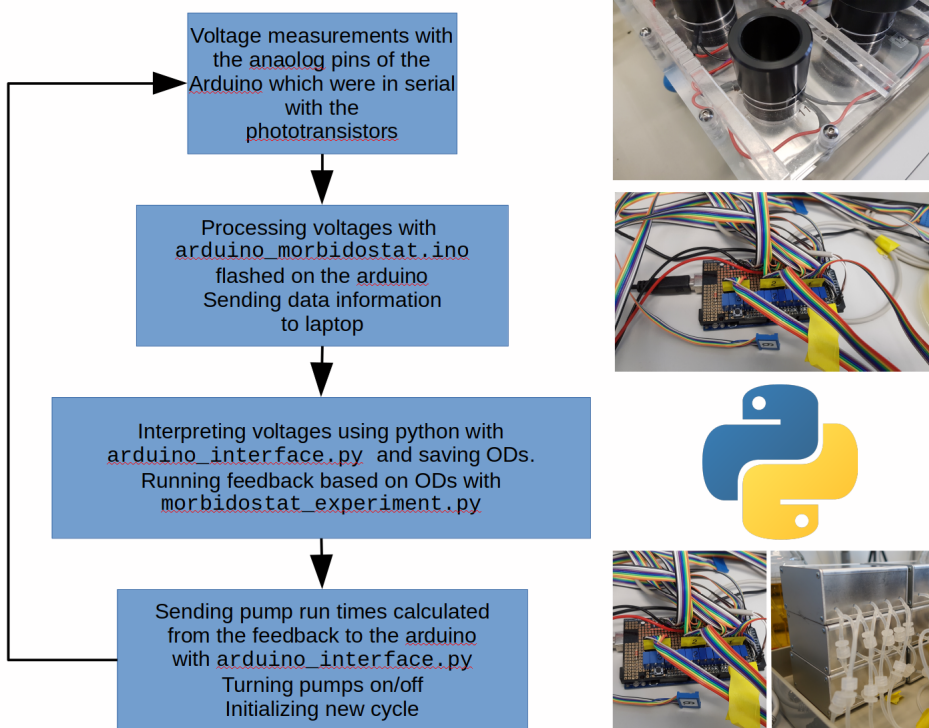


Figure 3.6: Overview of one cycle from the morbidostat.

commands received from the laptop. Those commands were measuring voltages of analog pins, needed for the OD measuring, or turning on/off digital pins which turned the pumps on/off (see section 3.3.1).

Command flow of the continuous mode

As for every mode the continuous mode consisted of several steps which were grouped in one cycle. Those cycles were constantly executed. As shown in Figure 3.6 the cycle itself was initialized by `morbidostat_experiment.py` and the ODs were measured and saved for every vial over the defined cycle time (typically 10 minutes).

Measuring of the OD as initialized by `morbidostat_experiment.py` led to a function call in `arduino_interface.py` which transmitted a command to the arduino. This command got interpreted and lead to measuring the voltages of the analog pins which were connected to an OD measuring unit as shown in top right of the Figure 3.6. The resulting voltages got transmitted to the `arduino_interface.py` via the serial communication. This script translated the voltages to ODs according to a linear equation defined earlier by calibration. `Morbidostat_experiment.py` was responsible for saving the ODs and averaging those values at the end of the cycle. As a next step a function in `morbidostat_experiment.py` calculated how much drug should get added to which vial, based on the recorded ODs. The output of the function were runtimes of certain pumps. Those runtimes were transmitted again to the arduino via the `arduino_interface.py` script and interpreted by the arduino. As shown in the last illustration of Figure 3.6 the arduino switched the according digital pins to high for the time communicated from the laptop.

Feedback of the continuous mode

The feedback coded as a function in morbidostat_experiment.py was very important since it was responsible for putting the culture under antibiotic pressure. The outcome of the feedback depended on the growth of the bacteria. Therefor the growth was calculated at the end of every cycle by calculating ΔOD according to the following formula:

$$\Delta OD = (final_OD[x_{cycles_back}] - final_OD[Cycle_{current}])/x$$

The final_OD was calculated at the end of every cycle by averaging every OD measurement gathered over one cycle. As shown in the equation the difference between the final_OD from the current cycle and the the final_OD of x cycles back (x being typically 10) was calculated and divided by x. As showin in Figure 3.7 the feedback did several comparisons before calculating an appropriate dose of drug. As a first step it checked if ΔOD was positive or negative. A negative ΔOD implied that the bacteria were dying. In order to prevent complete sterilization, media was getting added in this case.

When ΔOD was positive the bacteria were growing. Now it was important to not put the bacteria under selective pressure when the final_OD of the cultures was very small (e.g. 0.03). If drug was added at this stage, this usually led to complete sterilization. That's why a threshold was introduced which was called drug_dilution_threshold. Therefor the next comparison as visible in Figure 3.7 was whether or not the final_OD was higher or smaller than this threshold. If that was not the case the decision was to do nothing, which means that no fluid was added to the cultures.

However when the final_OD was bigger than the threshold calculation of the appropriate dose was started. This calculation depended on the MIC. Therefore the MIC had to be determined for the chosen bacteria and drug combination before the morbiostat experiment. Calculation of the concentration was divided into two equations consisting of an additive and a multiplicative component. The additive part was mainly important at the beginning of the experiment and was used to approximate a drug concentration in the vials similar to the MIC. Once the concentration in the vials was above the MIC the additive part was ignored. After that the current vial conentration was fed to an multiplicative equation. This equation multiplied the current drug concentration by the ΔOD which resulted in how much the drug concentration in the vial should be increased. This proved to be a good strategy, because fast growth meant stronger inhibition, but when the growth was very small and close to zero, the inhibition was not significantly increased. The multiplicative part also included other variables. For example a target_OD was defined which was used to define which OD should not be exceeded. In general it was the goal to have the OD of the cultures close and steady to the target_OD.

It was chosen to divide the outcome of the multiplicative component by this target_OD. Therefor if the target_OD was set to an high OD, inhibition was smaller than when set to a small OD. Furthermore variables had to be introduced to the multiplicative component which made it possible to make the feedback more aggressive or more sensitive.

Defining the target_OD was a trade off of having a higher probability of mutations for a higher defined target_OD, but keeping the culture at a high OD implemented fewer accuracy of the OD measurement caused by many dead cells.

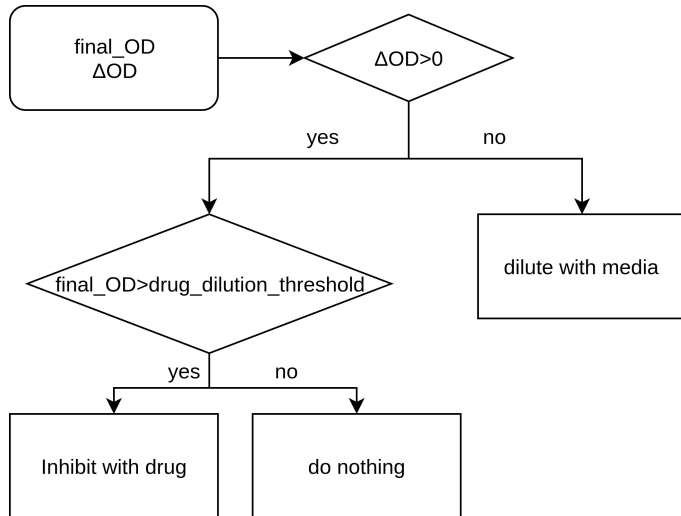


Figure 3.7: Schematic overview of decisions involved in the feedback

3.3.3 Hardware calibration

OD and pump calibration

We chose 1/10 LB media and 9/10 H_2O as a media for all experiments because the bacteria grew too fast when we used just LB media. All the culturing of the bacteria was done in a 37°C incubator.

For calibrating the OD measurements an overnight culture with K12 E. coli was inoculated in 5 ml diluted media. The next day the overnight culture was diluted 1/200 in 50 ml diluted media. After a few hours the OD of the culture was measured. Following OD standards were prepared with 18 ml diluted media in the vials for the morbidostat: 0.01 0.021 0.042 0.107 0.192 0.278

Then every vial with of a certain OD was placed in every vial holder. With the function calibrate_OD from the morbidostat_experiment.py script, a voltage measurement was done for every OD standard and every OD measuring unit. Because the voltage was measured for different ODs, the relation of voltage and OD could be described with a linear function.

For calibrating the pumps the function calibrate_pumps from the morbidostat_experiment.py was executed. This function demands the initial weight of every empty vial. After entering every weight, the function turned on every pump for 100 seconds. After that, the vials were weighted again and the values passed to the function which allowed precise calibration of each pump.

3.4 Safety aspects of morbidostat experiments

Every experiment was done within the hypoxi-station. Next to temperature and CO_2 and nitrogen composition control, this ensured that in case of a leak no pathogens would get out in the open.

Based on the clinical strains from the University hospital of Basel and the sequencing data we produced several plasmids which we transformed into K-12. From two patients patient25 and patient33 we isolated the sequences coding for CTX-M-1 and OXA from the most susceptible sample. Next to the sequence coding for the

ESBL we also took the upstream sequences up to the previous gene in order to ensure that we include the regulatory sequence. This resulted in three different plasmids. The patient number, ID of the plasmid and for which ESBL the sequence is coding is visible in Table 3.4. All the plasmids were produced by gibson cloning. Every resulting clone was Illumina sequenced by the University hospital of Basel.

Patient	Plasmid ID	ESBL
25	pEU22	CTX-M-1
25	pEU23	OXA
33	pEU26	OXA

Table 3.1: Produced plasmids

3.4.1 Gibson cloning

Primer design

3.5 Experimental procedure for culturing with the continuous mode

3.5.1 MIC determination

For experiments with the continuous mode the MIC of the antibiotic of interest had to be determined with the bacteria used for the experiment. That's because the feedback managing the inhibition is relied on the MIC.

Therefor 5 ml of MHB media was inoculated with the bacteria used for the actual experiment and cultured over night. The next day a 1/200 dilution in 20 ml MHB was prepared and cultured for a few hours. In the mean while a four fold concentration of the highest desired concentration was prepared. The growth of the diluted culture was constantly monitored by measuring the OD. When the OD of the diluted culture was at 0.08, a 1/100 dilution was done once again. From this final dilution 100 µl was pipetted in every well from the 96 well expect in the wells from the last column of the plate. Additionally 100 µl of MHB was added to every well. As a next step 100 µl from the prepared drug solution was added to the first column of the plate. Then 100 µl from this column were transferred to next column and mixed. This was repeated until the third last column. TThe second last column acted as a control of the cells, since no drug was added. The last column acted as a control for the media. After preparing the well plate it was incubated for 16 hours at 37 ° on a shaker. To get an idea how many cells were used for the MIC determination 10^{-3} and 10^{-5} dilutions of the 1/100 diluted cell suspension were plated on LB plates. After 16 hours the OD of every well was measured using a plate reader. The smallest concentration which inhibited the growth was determined as the MIC.

Determination of growth rates

For successfully culturing in the continuous mode appropriate dilution was helpful. A rather high dilution was helpful because an exchange of fluid prevented that too many bursted cell parts accumulated in the culture. Furthermore having a higher

dilution helped to prevent the cultures from overgrowing. This was particularly useful at the beginning of the experiment because there was a lag until the antibiotic inhibited the growth. In order to determine an appropriate dilution it was necessary to record the growth rates of bacteria used for the experiment. Therefore all the growth rates were determined by culturing the bacteria used for the experiments in the GROWTH_RATE_EXPERIMENT mode. The recorded growth rates were then fed to the morbidostat_simulator.py script. This allowed to test different dilutions and to choose an appropriate cycle time.

Sterilization of the morbidostat

Before the experiment in the continuous mode could be started the morbidostat had to be sterilized. In order to do so all the tubing was flushed with 1 L of 3 % citric acid, followed by 1 L of sterile water. After that 1 L of 3 % bleach and 1 L of water was pumped through the tubing. All the media, drug bottles and vials including luer connections were autoclaved before the experiment.

3.5.2 Testing the feedback from the continuous culture mode

An overnight culture was set up by inoculating 5 ml of diluted media with K12 XL1-Blue E. coli. The next day a 1/200 dilution in 200 ml was prepared and 18 ml of this suspension was pipetted in 18 sterile vials.

As described in 3.5.1 the growth rates of K12 were determined over night and ideal dilution and cycle times tested with the simulator. A dilution factor of 0.94 and a cycle time of 12 minutes were chosen. As a drug we used amoxicillin, its MIC was determined as 2 μ /ml according to the procedure in 3.5.1. As a starting concentration 6 μ /ml and 14 μ /ml were chosen for the drug bottles. Tubing, bottles and vials were sterilized according to the section 3.5.1. From an other overnight culture of K12 XL1-Blue E. coli in 5 ml diluted media the morbidostat experiment was started in the continuous mode. Therefor the cells were diluted to an OD of 0.015 in 18 ml. Every other day 200 μ l of the suspension in the vials were transferred into new sterile vials filled with 18 ml diluted media. When a drug bottle was empty, the MIC was changed in the morbidostat_experiment.py according to the concentration which was needed to strongly inhibit the growth. New drug concentrations were chosen based on the newly determined MIC. For the lower concentrated bottle a 3 fold MIC concentration, was chosen. For the higher concentrated drug bottle the concentration was set to 7 fold MIC. At day 4 of the experiment, samples were taken from every vial, by opening the vial in the hypoxi-station and transferring 200 μ l into eppendorf tubes. Those samples were cultured over night in 5 ml diluted media and the next day the MIC was determined. The morbidostat experiment was stopped after 6 days.

3.5.3 Culturing K12 carrying ESBL plasmids with the morbidostat

With the clones carrying ESBL plasmids (see Section 3.4.1) we ran two continuous morbidostat experiments. Over night cultures of every clone were prepared in 3 ml LB with 3 μ L kanamycine. K12 was cultured over night in just 3 ml LB. The

over night culture was diluted 200 fold the next day and the growth rates were determined (see Section 3.5.1). Additionally the MICs of every clone and K12 were determined as 2 µg/ml (see Section 3.5.1). Based on the growth rates the dilution factor was set to 0.91 and the cycle time to 10 minutes. As drug concentrations 9 µg/ml and 21 µg/ml were chosen. MIC and drug concentrations were changed as described in Section 3.5.2. The experiment was started with a starting OD of every culture of 0.015. From every different clone a control was cultured where no antibiotic pressure was applied and the cultures were diluted with media to a fixed OD. This fixed OD (target_OD) was set to 0.12. Different modes were chosen for following vials.

Vial	Plasmid	Mode
1	pEU26_OXA	continuous
2	pEU26_OXA	continuous
3	pEU23_OXA	continuous
4	pEU23_OXA	continuous
5	pEU23_OXA	continuous
8	pEU26_OXA	continuous
9	pEU23_OXA	fixed OD

Vial	Plasmid	Mode
1	pEU26_OXA	continuous
2	pEU23_OXA	continuous
3	pEU22_CTX-M-1	continuous
4	pEU22_CTX-M-1	continuous
5	pEU22_CTX-M-1	continuous
7	K12	continuous
8	pEU22_CTX-M-1	fixed OD
9	pEU26_OXA	fixed OD
10	pEU26_OXA	fixed OD

Table 3.2: Left table: Experiment 01, right table: Experiment 02

Experiment 01 ran for two days and only samples were taken from the last day. Experiment 02 ran for six days and samples were collected every day. For sampling 1 ml of every vial was transferred into an eppendorf tube within the hypoxi-station. The samples was centrifuged for 10 minutes at 13000 rpm and the resulting cell pellet resuspended in 200 µLB media containing 20 % glycerol. The resuspended cells were frozen and kept as stocks.

From the 01 experiment the stocks of every vial from the last sample day were handed over to the University hospital of Basel for Illumina sequencing. From the 02 experiments samples from the second sample day of vial 3,4,5,7 and 8 were chosen for sequencing. Additionally every sample from the last sampling day of the 02 experiments were handed over for Illumina sequencing.

Chapter 4

Results

4.1 Analyzing ESBL E. coli isolates from patients of the University hospital Basel

4.1.1 Sample selection

The sample collection consisted of 65 samples screened positive for ESBL genes coming from 34 patients. An identifier was created for each sample consisting of the patient number and the sample number. Sample numbers chronologically increased meaning that sample 0 was the first sample collected from a patient. From the 34 patients we had to select for patients which were suitable for our analysis. Obviously multiple samples per patient were necessary which was not the case for 15 patients. In order that SNPs could be identified which were likely associated with resistance it was necessary that the samples collected from one patient were the same ESBL E. coli strain. By building a phylogenetic tree of all the samples we could check how closely related different samples were.

Pylogeneic analysis with panX

Only patients could be used for the analysis where every sample mapped on the same branch on the phylogenetic tree created with PanX. If that was the case the samples shared the identical core genomes. Samples of one patient mapping on different branches imply that their core genome differed and they were different strains. Therefore the patient was infected with different strains over the sample period which made it impossible for us to identify SNPs potentially involved in the resistance mechanism.

From the 19 patients with multiple samples 7 patients had samples which mapped on different branches. This is visible in Figure 4.1. For example patient 15 had two samples which mapped on two different clades of the tree. Those 7 patients had to be excluded from the analysis as well.

It's also visible in Figure 4.1 that some samples from different patients map on the same branch. This tells us, that some patients were infected by the same strain coming probably from the same outbreak within the hospital. On the other hand patient 25 has two samples which map on a separate clade of the phylogenetic tree. This indicates that this patient most likely got infected outside the hospital.

What also reduced the patients which could be used for the analysis was that

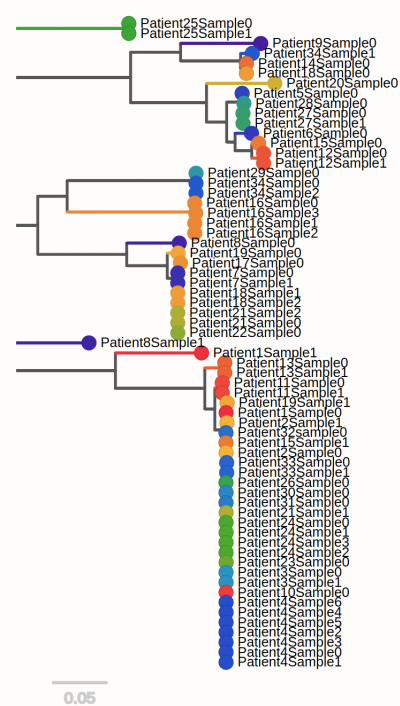


Figure 4.1: Phylogenetic tree built with panX. The samples are colored by the patient.

not all of them had a significant increase or decrease of the MIC for cefepime or ceftazidime. Since those MIC were determined by a 2-fold dilution series it was not enough when the concentration doubled over time. This reduced the selection to 5 patients. The meta data and the MIC for those patients are shown in Table 4.1.

4.1.2 Sequencing and assembling

Ever sample shown in Table 4.1 was successfully sequenced with a MinION from Oxford Nanopore Technologies. From each patient a reference genome was successfully built for the sample with the lowest MIC. The selected sample for building the reference genome is shown stained in cyan in Table 4.1. Note that for patient 24 sample 0 was selected even though technically sample 2 has lower MICs. But since the MIC from those samples are very similar we decided to choose sample 0 because it was collected the earliest.

As shown in Table 4.2 the lowest coverage for a sequenced sample which was used to build a reference genome was 73. All the other samples had a coverage of higher than 200, but even 73 is more than sufficient. The last column of Table 4.2 shows how many contigs were detected by Unicycler. Note that a hybrid assembly was used to build the reference genome, which means that the long-reads from Nanopore were supplemented with short-reads from Illumina.

4.1.3 SNPs

Mapping all the short-reads from one patient to the according reference genomes revealed about 100 SNPs for all patients. Those SNPs had a short-read coverage of at least 30 and a minimum base frequency of 0.8.

Only SNPs with annotation are presented in the following tables. All the tables with

Accession	Sample date	MIC Cefepim	MIC Cefepim	Sandra	Ceftazidim
Patient12Sample0	9.9.14	4	16	0.75	
Patient12Sample1	5.12.14	12	32	2	
Patient16Sample0	22.6.12	8	32	2	
Patient16Sample1	18.7.13	48	64	8	
Patient16Sample2	1.11.13	32	32	12	
Patient24Sample0	02.05.11	4	16	1.5	
Patient24Sample1	08.15.11	16	32	1.5	
Patient24Sample2	11.28.11	3	8	1	
Patient25Sample0	15.4.11	64	None	192	
Patient25Sample1	22.8.11	6	4	6	
Patient33Sample0	26.9.14	24	None	16	
Patient33Sample1	29.1.15	1	2	1.5	

Table 4.1: Those patients have been selected because their samples differ significantly in MIC and mapped on the same branch in panX. The samples which are stained in cyan were chosen for building the reference genome.

Accession	Total gigabases sequenced	Coverage	Assembled in n contigs
Patient12Sample0	0.39	73	6
Patient16Sample0	1.11	207	3
Patient24Sample0	1.81	336	17
Patient25Sample1	1.82	338	12
Patient33Sample1	1.24	231	6

Table 4.2: Total sequenced bases and resulting coverage for every sample which was chosen for building a reference genome. The coverage was calculated by assuming the genome size of E. coli is 5.4 megabases. the last column displays into how many contigs the genome was devided by the assembler Unicycler.

SNPs with gene annotation share the same structure. The first column describes in which sample the SNP was identified. The columns "gene" and "product" describe what gene and transcribed protein is affected by the SNP. The last column shows at which position of the gene the SNP caused a change of the amino acid. The first amino acid is the one found in the reference sample. The second amino acid is the changed amino acid in the resistant sample caused by the SNP. Only for patient 16 SNPs were found with promoter annotation. The SNPs with no annotation are listed for all patients in the supplementary (see Section 6.2)

Patient 12

For patient 12 no SNPs with annotation were found. In total 4 SNPs were identified for this patient.

Patient 16

In Table 4.3 every SNP for this patient is shown where a gene annotation was found. All of the SNPs for this patient were found on the chromosome. In total we detected 46 SNPs for this patient.

Accession	Gene	Product	Position and change of AA
Sample1	ortT	Orphan toxin OrtT	44: P → T
Sample1	scrY	Sucrose porin	104: L → V
Sample1	cpdA	Phosphodiesterase	116: Deletion, length: 1
Sample2	cpdA	Phosphodiesterase	116: Deletion, length: 1
Sample1	rpoB	RNA polymerase subunit	113: V → I
Sample1	ftsQ	Cell division protein FtsQ	207: K → R
Sample1	recR	Recombination	40: M → T
Sample1	hcxA	Dehydrogenase A	332: R → G
Sample1	ribA	GTP cyclohydrolase-2	68: F → L

Table 4.3: Every SNP for patient 16 which affected a gene. Three nucleotides were deleted in cpdA therefor no frame-shift was caused.

For this patient some SNPs were identified which affected promotores. Two promotores were identified with the promotor prediction tool PePPER and one promotor was identified based on the promotor data base hosted on EcoCyc [41]. Every SNP affecting an identified promotor is shown in Table 4.4.

Accession	Position of SNP and change of base	Next upstream gene
Sample1	2295830: A → C	2295954: dcuD_1
Sample2	2295830: A → C	2295954: dcuD_1
Sample1	2437088: A → G	2437306: ISEc1
Sample1	4333944: G → A	4333792: fepA:

Table 4.4: The second column shows the position of the SNP and the change of the nucleotide. The SNP colored with cyan affected a promotor which was identified based on EcoCyc. The others are based on the promotor preidction tool PePPER.

Figure 4.1.3 shows the alignment of the sequences concerning the SNP in the promotor of fepA. This is the promotor which was identified with EcoCyc. The mutation was found in the binding site of the σ 70 transcription factor.

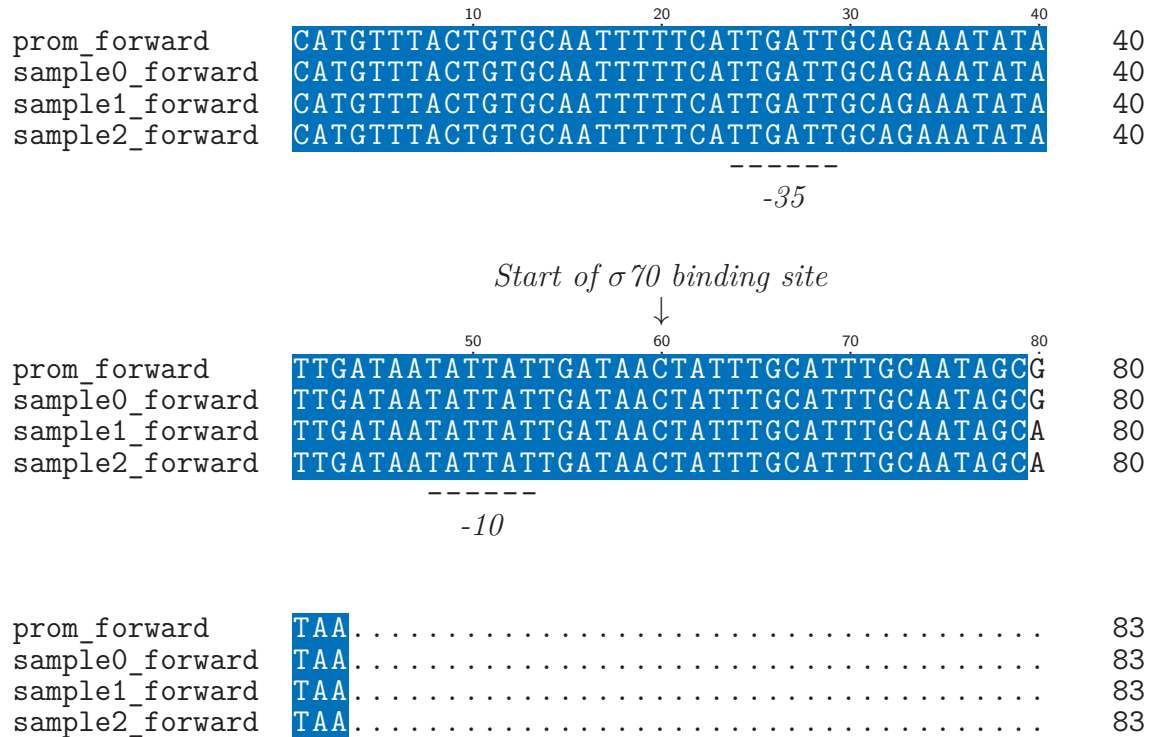


Figure 4.2: This alignment shows the SNP in the fepA promotor. Positions marked with the dashed line are the recognition sites for σ 70 factor.

Patient 24

For patient 24 several SNPs with gene annotation were identified, all of them on the chromosome.

Accession	Gene	Product	Position and change of AA
Sample1	atl	DNA base-flipping protein	87: V → M
Sample1	Imm_2	Colicin-E7 immunity protein	69: K → E
Sample1	lldR_2	Dehydrogenase operon regulatory protein	44: I → S 1
Sample2	lldR_2	Dehydrogenase operon regulatory protein	44: I → S 1
Sample1	dctM_2	TRAP transporter large permease protein	112: T → S S
Sample2	dctM_2	TRAP transporter large permease protein	207: T → S
Sample1	dltA	D-alanine-poly ligase subunit 1	692: E → G
Sample1	fnr	Reduction regulatory protein	31: C → F
Sample2	fnr	Reduction regulatory protein	31: C → F

Table 4.5: Every SNP for patient 24 which affected a gene.

Patient 25

For patient 25 only two SNPs were identified with gene annotation.

Accession	Gene	Product	Position and change of AA
Sample0	envZ	Osmolarity sensor protein EnvZ	87: V → M
Sample0	rfbD	dTDP-4-dehydrorhamnose reductase	148: Deletion, length: 4

Table 4.6: Every SNP for patient 25 which affected a gene. In rfbD a the nucleotide length of the deletion was 12 and therefore no frame-shift was caused.

Patient 33

Also only two SNPs with gene annotation were found for patient 33.

Accession	Gene	Product	Position and change of AA
Sample0	cydD	ATP-binding/permease protein CydD	368: L → Q
Sample	vnfA	Nitrogen fixation protein VnfA	169: I → N

Table 4.7: Every SNP for patient 33 which affected a gene.

Comparing the coverage of sample 0 and sample 1 revealed that there is a significant increase of coverage for a region of sample 0. As seen in Figure 4.3 this region is about 17 kbp long and an ESBL gene is located within this area. The ESBL gene annotated as bla_2 is coding for the CTX-M-1 β -lactamase. Bla_1 at the boarder of the region is not included anymore and shows a normal coverage of around 30.

So many more reads mapping to this region in sample 0 imply that this region is present multiple times. This is possible if the region is located on a separate plasmid which is present in amplified copy numbers. It's also possible that this region is present multiple times on the same plasmid.

Studying the assembly for sample 0 produced with unicycler didn't answer this question. No increased copy number could be found within this assembly. But hybrid-assembling the short- and long-reads with canu and pilon revealed that 9 CTX-M-1 genes were present in this sample. For control sample 1 was assembled using canu but identical to Unicycler only one CTX-M-1 gene were found.

4.1.4 Comparing ESBL genes in the resistant samples and the susceptible samples

Since we long-read sequenced every sample from Table 4.1 we hybrid-assembled and annotated those samples as well. This allowed us to see what ESBL genes were present in the susceptible and the resistant samples. The present ESBL genes and their copy numbers are shown in Figure 4.5. Except for patient 33 there was no significant change in the copy numbers. But interestingly many strains lost or took up new ESBL genes over time.

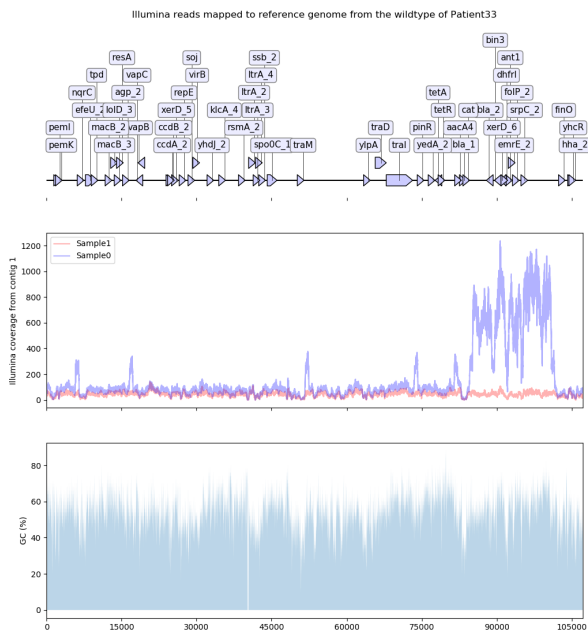


Figure 4.3: Upper figure: Annotation of the whole plasmid. Middle figure: Coverage of the illumina sequencing data from sample 0 (resistant sample) and sample 1 (susceptible sample). Bottom figure: GC content.

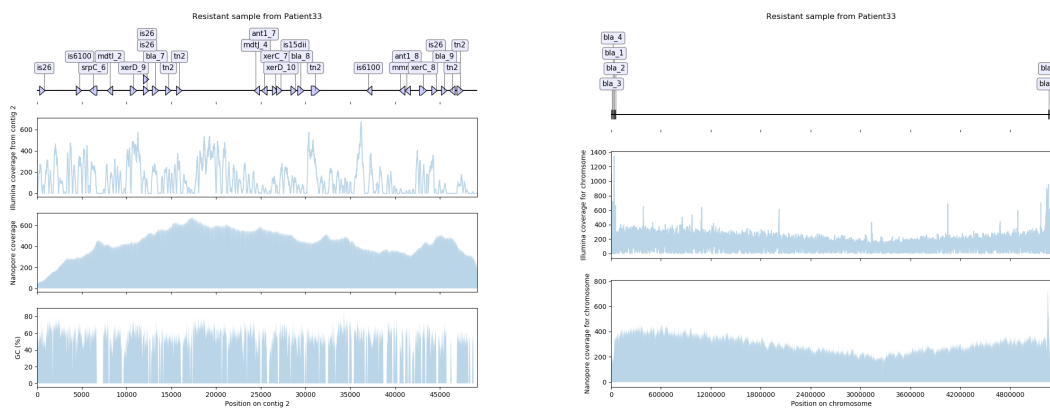


Figure 4.4:

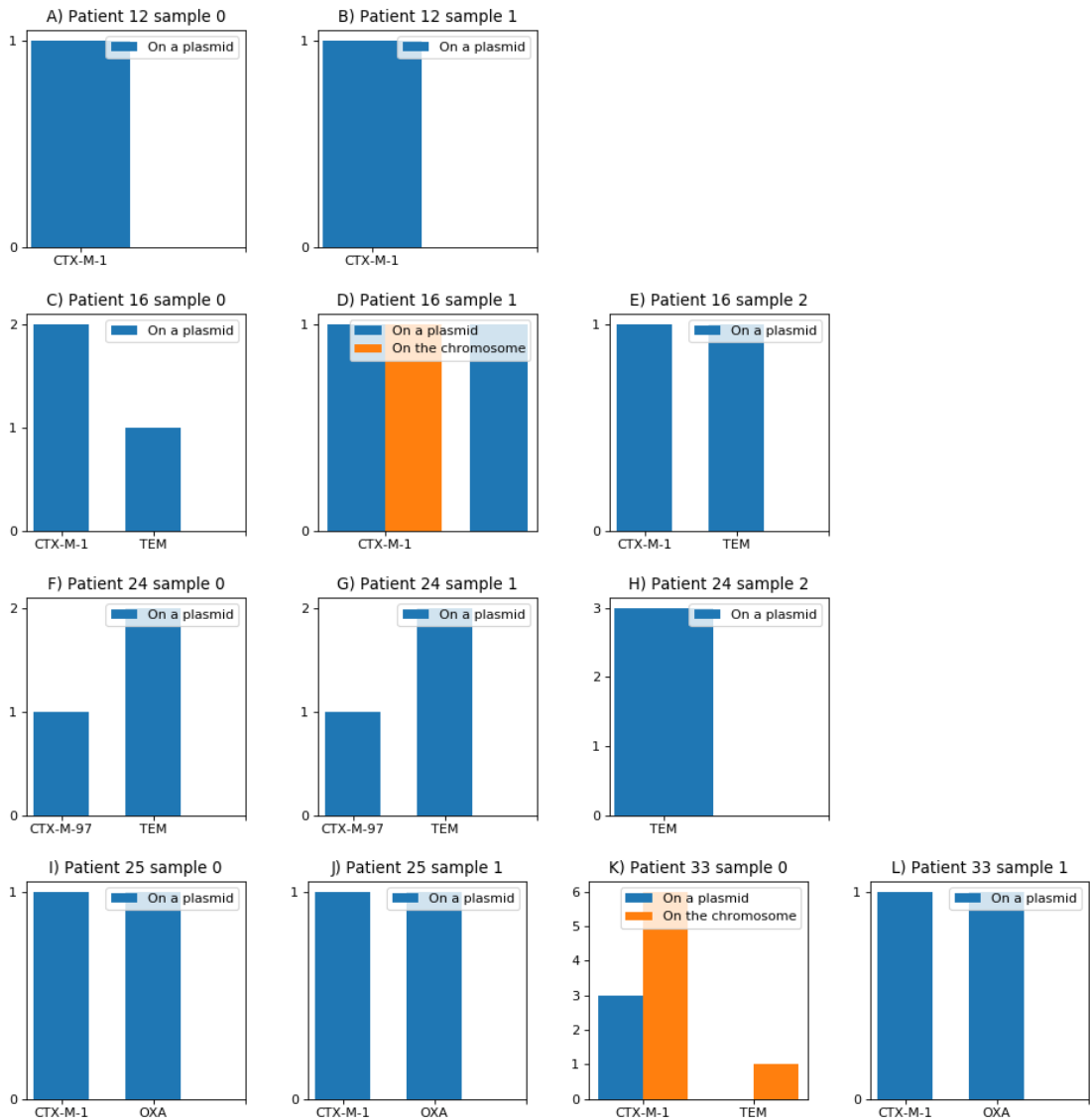


Figure 4.5: Copy numbers of ESBL genes. A-B: Patient 12, sample 1 resistant. C-E: Patient 16, sample 1 and 2 resistant. Change of copy number of CTX-M-1 and TEM. F-H: Patient 24, sample 1 resistant. CTX-M-97 was lost over time, increase of TEM copy number. I-J: Patient 25, sample 0 resistant. K-L: Patient 33 sample - resistant. Resistant sample has 8 more copies of CTX-M-1 where most of the copies are located on the chromosome.

4.2 Morbidostat experiments

4.2.1 Testing the continuous experiment

The MIC of amoxicillin was determined as 2000 ng/ μ l. The grow curve which was recorded before the initial experiment is shown in Figure 4.6. It's visible that the growth slows down at an OD of 0.3, which is because 10 fold diluted media was used. The ODs and amoxicillin concentrations for the continous morbidostat experiment are shown in Figure 4.7. Measuring of the OD for vial 1 behaved weirdly for the first

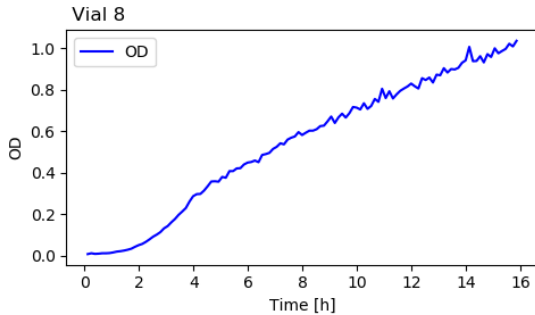


Figure 4.6: Grow curve of XL1 blue E. coli with 10 fold diluted LB media

10 hours. This was caused by wrong calibration of the OD measuring unit, causing problems of detecting the right OD at low ODs. At around 40 hours 200 μ l of every cell susepnsion was transferred into 18 ml of new diluted media. It's visible that the accuracy of the OD measurement decreased before this dilution. That's because many dead cells caused scattering of the light which falsifies the OD measurement. In the second half of the experiment the drug concentrations were very high. Somehow the high amoxicillin concentration led to milky suspension when injected to the vials. This explanis why the OD measurements were more fuzzy towards the end. Also we observed that dead cells formed filament like aggregations. By stirring this sometimes caused wrong OD measurements as visible for vial 6 in Figure 4.7 at the end of the experiment. The morbidostat reacted very well to the detected growth of every vial. The target OD was set to 0.15 and every vial approximated this OD over time. Furthermore the algorithm reacted well by diluting with media when the cells died, or by increasing the drug concentration when the cells grew fast.

To get a better idea how the feedback reacted the first 40 hours of vial 8 are shown enlarged in Figure 4.7. In this Figure it's visibile that no drug was injected until the OD of the vial was higher than the the drug_dilution_threshold (0.7). After that the amoxicillin concentration was constantly increased until the cells started to die. At the point where the OD decreased the concentration was stored which was 2000 ng μ /ml which is the same value as the MIC determined before the experiment. While the cells were dying media was added until the concentration was a quarter of the concentration which was necessary to kill the cells. With the cells starting to grow again, the drug concentration was increased up to the point where the cells started to die again. As visible in the Figure 4.8 double of the MIC was necessary to kill the cells this time.

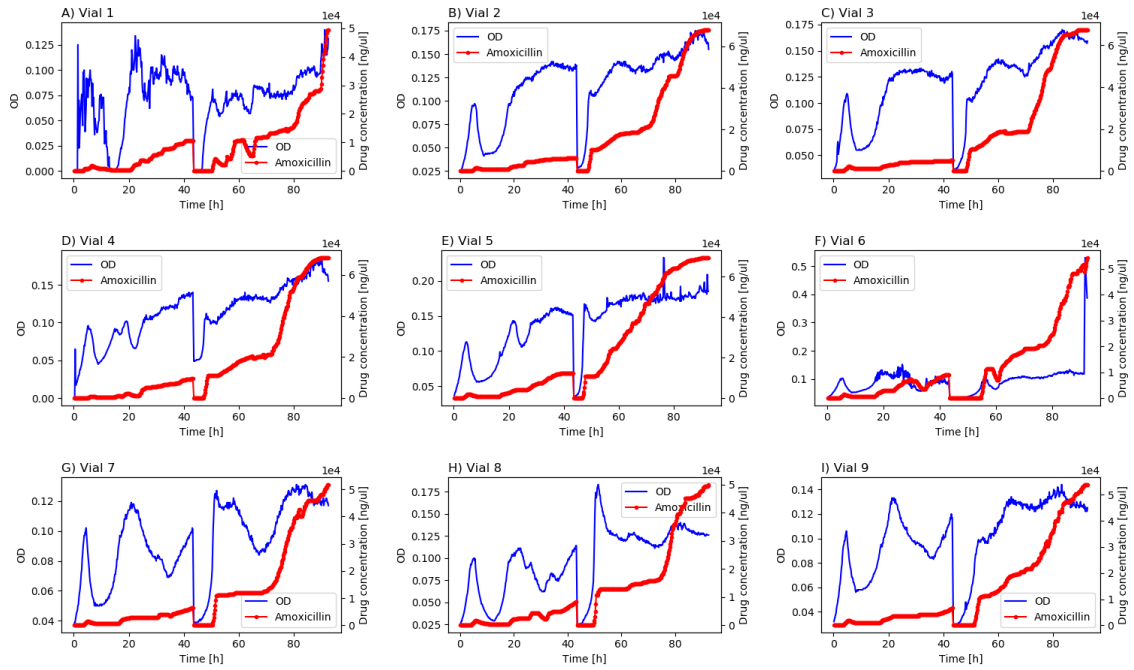


Figure 4.7: For the continuous morbidstat experiment we cultured XL1 blue E. coli in 9 vials. Each plot shows the OD and the amoxicillin concentration for each vial over the whole experiment time (4.5 days). Dilution factor was 0.94, cycle time 12 minutes and the target OD 0.15. The kink in the OD and drug concentrations at 42 hours comes from transferring 200 μ l into new diluted media.

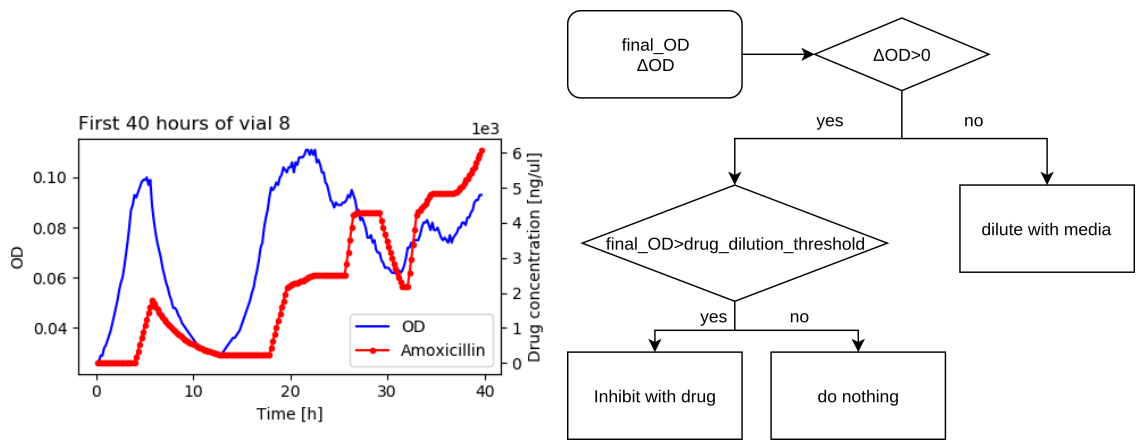
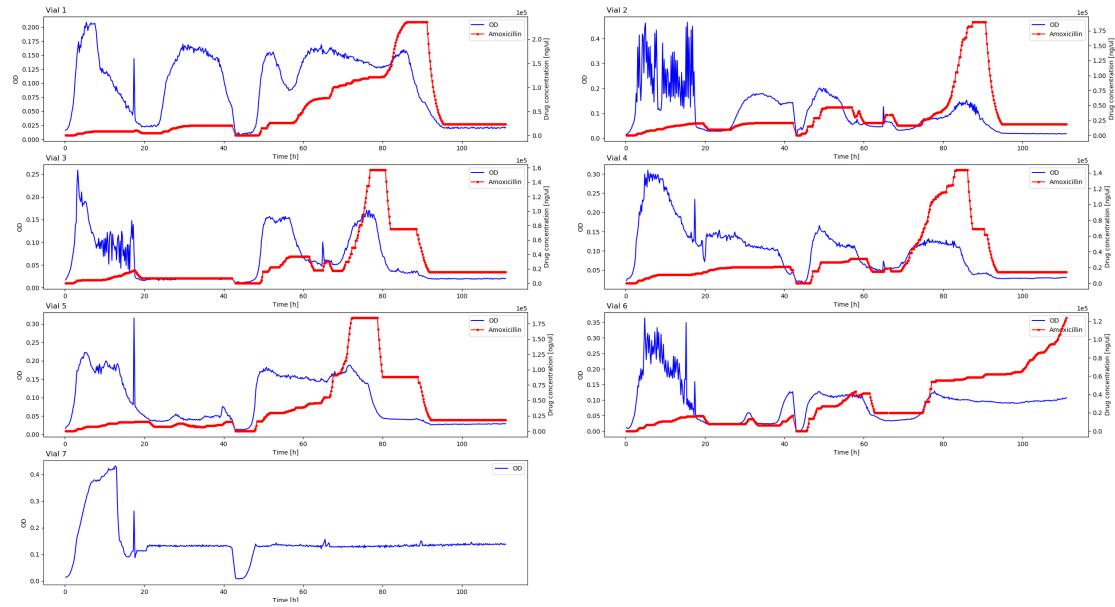
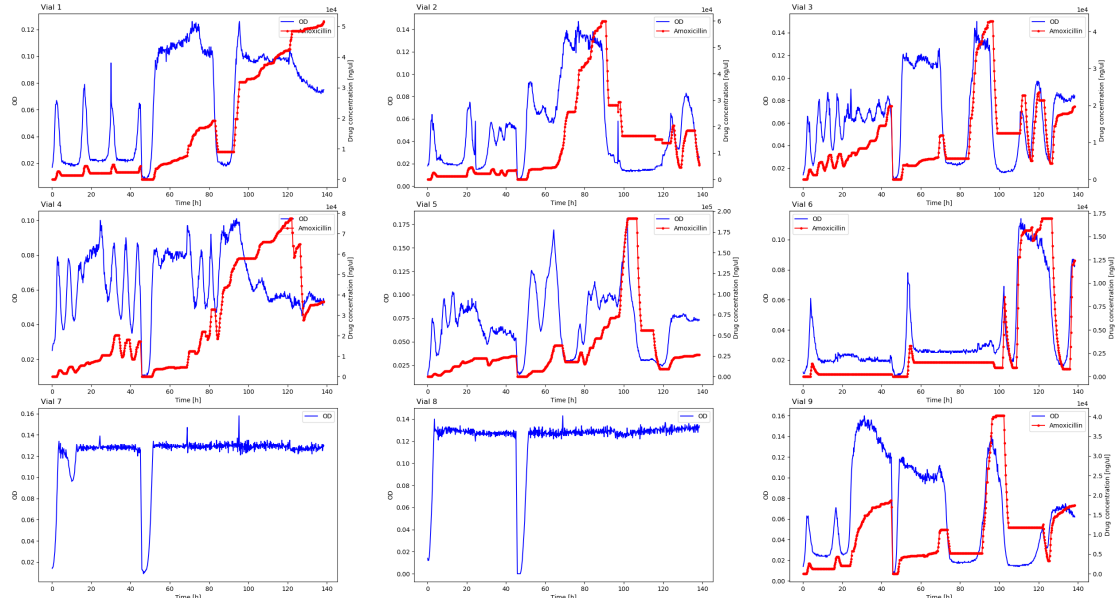


Figure 4.8: Left: First 40 hours of vial 8 from the continuous morbidostat. For the whole experiment time see Figure 4.7. Right: Feedback algorithm deciding over drug injections.

4.2.2 Morbidostat experiment 01



4.2.3 Morbidostat experiment 02



Chapter 5

Discussion

5.1 Analysis of the ESBL *E. coli* patient isolates

5.1.1 SNPs

We identified several SNPs altering genes and promoters for four out of 5 analyzed patients. By studying the literature we try to make connections to the altered genes and other already studied resistance mechanisms.

orT coding for orphan toxin is an inner-membrane protein which is activated under conditions inducing stringent response [22]. By damaging the cell membrane and reducing the intracellular ATP level cell growth is reduced. OrtT can increase persistence, a state in which cells are tolerant to antibiotics [22]. Islam et al. showed that expression of ortT increases up to 80 fold when the cells are put under antibiotic pressure. None of the testes antibiotics were β -lactams.

scrY

Knowing mutations which play a key factor in gaining resistance would allow to predict resistance of ESBL *E. coli* based on genomic information.

Chapter 6

Supplementary

6.1 Manual for starting experiments with morbidostat

6.2 SNPs with no annotation

Patient12			
Contig	Position	Samples	
0	880249	Sample0: C	Sample1: A
0	1619787	Sample0: G	Sample1: A
0	2481354	Sample0: A	Sample1: G
0	4256761	Sample0: A	Sample1: T

Patient16				
Contig	Position	Samples		
0	55597	Sample0: A	Sample1: G	Sample2: G
0	387261	Sample0: C	Sample1: A	Sample2: C
0	387282	Sample0: A	Sample1: C	Sample2: C
0	420182	Sample0: T	Sample1: C	Sample2: T
0	420183	Sample0: G	Sample1: A	Sample2: G
0	539392	Sample0: G	Sample1: A	Sample2: A
0	808891	Sample0: C	Sample1: T	Sample2: T
0	813579	Sample0: T	Sample1: A	Sample2: T
0	813613	Sample0: C	Sample1: A	Sample2: C
0	813614	Sample0: C	Sample1: A	Sample2: C
0	893946	Sample0: C	Sample1: A	Sample2: C
0	922702	Sample0: G	Sample1: A	Sample2: G
0	1133762	Sample0: C	Sample1: T	Sample2: T
0	1508583	Sample0: A	Sample1: T	Sample2: T
0	1508592	Sample0: A	Sample1: T	Sample2: T
0	1508611	Sample0: -	Sample1: T	Sample2: T
0	1508618	Sample0: A	Sample1: T	Sample2: T
0	1508625	Sample0: A	Sample1: C	Sample2: C
0	1525597	Sample0: A	Sample1: G	Sample2: A

0	1549518	Sample0: T	Sample1: G	Sample2: G
0	1729351	Sample0: A	Sample1: C	Sample2: C
0	2016331	Sample0: A	Sample1: C	Sample2: A
0	2023731	Sample0: A	Sample1: T	Sample2: A
0	2101129	Sample0: C	Sample1: -	Sample2: -
0	2101130	Sample0: A	Sample1: -	Sample2: -
0	2128255	Sample0: T	Sample1: -	Sample2: T
0	2531373	Sample0: -	Sample1: T	Sample2: T
0	2647199	Sample0: T	Sample1: C	Sample2: T
0	2798262	Sample0: T	Sample1: C	Sample2: T
0	2798288	Sample0: T	Sample1: C	Sample2: T
0	2798294	Sample0: T	Sample1: A	Sample2: T
0	2798312	Sample0: A	Sample1: C	Sample2: C
0	3503181	Sample0: A	Sample1: T	Sample2: T
0	3920934	Sample0: A	Sample1: G	Sample2: A
0	4459680	Sample0: C	Sample1: -	Sample2: C
0	4459681	Sample0: C	Sample1: -	Sample2: C
0	4459684	Sample0: G	Sample1: -	Sample2: G
0	4459685	Sample0: A	Sample1: -	Sample2: A
0	4459686	Sample0: A	Sample1: -	Sample2: A
0	4459687	Sample0: G	Sample1: -	Sample2: G
0	4459688	Sample0: A	Sample1: -	Sample2: A
0	4459689	Sample0: G	Sample1: -	Sample2: G
0	4459692	Sample0: A	Sample1: -	Sample2: A
0	4459693	Sample0: G	Sample1: -	Sample2: G
0	4459695	Sample0: G	Sample1: -	Sample2: G
0	4459697	Sample0: T	Sample1: -	Sample2: T
0	4842004	Sample0: C	Sample1: T	Sample2: T

Patient24				
Contig	Position	Samples		
0	418566	Sample0: T	Sample1: C	Sample2: T
0	418588	Sample0: G	Sample1: A	Sample2: G
0	1505822	Sample0: C	Sample1: A	Sample2: A
0	1505825	Sample0: A	Sample1: T	Sample2: T
0	1925913	Sample0: A	Sample1: C	Sample2: C
0	1925915	Sample0: A	Sample1: T	Sample2: T
0	2925037	Sample0: C	Sample1: T	Sample2: T
0	2954867	Sample0: C	Sample1: T	Sample2: T

Patient25			
Contig	Position	Samples	
0	1998615	Sample0: T	Sample1: A
0	3480363	Sample0: T	Sample1: C
0	3743644	Sample0: A	Sample1: G
0	4785433	Sample0: G	Sample1: A

0	4785439	Sample0: G	Sample1: A
---	---------	------------	------------

Patient33			
Contig	Position	Samples	
0	2887411	Sample0: A	Sample1: C

Chapter 7

Declaration

asdfaggj

Chapter 8

References

Bibliography

- [1] Erdal Toprak et al. “Building a Morbidostat: An automated continuous-culture device for studying bacterial drug resistance under dyna-ally sustained drug inhibition”. In: *PMC* (2013).
- [2] Nicholas Noll et al. “Prokka: Resolving structural diversity of Carbapenemase-producing gram-negative bacteria using single molecule sequencing”. In: *bioarchive* (2018).
- [3] *Antibiotic Use in the United States, 2017: Progress and Opportunities — Antibiotic Use — CDC*. Jan. 23, 2019. URL: <https://www.cdc.gov/antibiotic-use/stewardship-report/outpatient.html> (visited on 06/13/2019).
- [4] *Antibiotikaresistenzen*. Mar. 27, 2019. URL: <https://www.bag.admin.ch/bag/de/home/krankheiten/infektionskrankheiten-bekaempfen/antibiotikaresistenzen-welche-bakteriellen-krankheiten-gibt-es-.html>.
- [5] *Babraham Bioinformatics - Trim Galore!* URL: https://www.bioinformatics.babraham.ac.uk/projects/trim_galore/ (visited on 04/15/2019).
- [6] Hélène Barreteau et al. “Cytoplasmic steps of peptidoglycan biosynthesis”. In: *FEMS Microbiology Reviews* 32.2 (Mar. 1, 2008), pp. 168–207. ISSN: 0168-6445. DOI: 10.1111/j.1574-6976.2008.00104.x. URL: <https://academic.oup.com/femsre/article/32/2/168/2683919> (visited on 04/29/2019).
- [7] *beta-lactam antibiotic*. In: *Wikipedia*. Page Version ID: 883614313. Feb. 16, 2019. URL: https://en.wikipedia.org/w/index.php?title=%CE%92-lactam_antibiotic&oldid=883614313 (visited on 04/09/2019).
- [8] *Beta-Lactam Antibiotics - an overview — ScienceDirect Topics*. URL: <https://www.sciencedirect.com/topics/neuroscience/beta-lactam-antibiotics> (visited on 04/17/2019).
- [9] *Beta-Lactam Ring - an overview — ScienceDirect Topics*. URL: <https://www.sciencedirect.com/topics/chemistry/beta-lactam-ring> (visited on 04/17/2019).
- [10] Patricia A. Bradford. “Extended-Spectrum β -Lactamases in the 21st Century: Characterization, Epidemiology, and Detection of This Important Resistance Threat”. In: *Clinical Microbiology Reviews* 14.4 (Oct. 2001), p. 933. DOI: 10.1128/CMR.14.4.933-951.2001. URL: <https://www.ncbi.nlm.nih.gov/pmc/articles/PMC89009/> (visited on 04/17/2019).
- [11] CDC. *The biggest antibiotic-resistant threats in the U.S.* Centers for Disease Control and Prevention. Mar. 27, 2019. URL: https://www.cdc.gov/drugresistance/biggest_threats.html (visited on 04/17/2019).

- [12] Peter J. A. Cock et al. “Biopython: freely available Python tools for computational molecular biology and bioinformatics”. In: *Bioinformatics* 25.11 (June 1, 2009), pp. 1422–1423. ISSN: 1367-4803. DOI: 10.1093/bioinformatics/btp163. URL: <https://academic.oup.com/bioinformatics/article/25/11/1422/330687> (visited on 04/16/2019).
- [13] *Colistin: An Update on the Antibiotic of the 21st Century*. Medscape. URL: <http://www.medscape.com/viewarticle/772588> (visited on 04/15/2019).
- [14] Sean R. Connell et al. “Ribosomal Protection Proteins and Their Mechanism of Tetracycline Resistance”. In: *Antimicrobial Agents and Chemotherapy* 47.12 (Dec. 1, 2003), pp. 3675–3681. ISSN: 0066-4804, 1098-6596. DOI: 10.1128/AAC.47.12.3675-3681.2003. URL: <https://aac.asm.org/content/47/12/3675> (visited on 04/29/2019).
- [15] S. J. Dancer. “The problem with cephalosporins”. In: *Journal of Antimicrobial Chemotherapy* 48.4 (Oct. 1, 2001), pp. 463–478. ISSN: 0305-7453. DOI: 10.1093/jac/48.4.463. URL: <https://academic.oup.com/jac/article/48/4/463/700308> (visited on 04/17/2019).
- [16] Wei Ding, Franz Baumdicker, and Richard A Neher. “panX: pan-genome analysis and exploration”. In: *Nucleic Acids Research* 46.1 (Jan. 9, 2018), e5. ISSN: 0305-1048. DOI: 10.1093/nar/gkx977. URL: <https://www.ncbi.nlm.nih.gov/pmc/articles/PMC5758898/> (visited on 04/15/2019).
- [17] Bianca Döbelmann et al. “Rapid and Consistent Evolution of Colistin Resistance in Extensively Drug-Resistant *Pseudomonas aeruginosa* during Morbidostat Culture”. In: *Antimicrobial Agents and Chemotherapy* 61.9 (2017). ISSN: 1098-6596. DOI: 10.1128/AAC.00043-17.
- [18] Richard J. Fair and Yitzhak Tor. “Antibiotics and bacterial resistance in the 21st century”. In: *Perspectives in Medicinal Chemistry* 6 (2014), pp. 25–64. ISSN: 1177-391X. DOI: 10.4137/PMC.S14459.
- [19] Rúben Fernandes, Paula Amador, and Cristina Prudêncio. “ β -Lactams: chemical structure, mode of action and mechanisms of resistance”. In: *Reviews in Medical Microbiology* 24.1 (Jan. 2013), pp. 7–17. ISSN: 0954-139X. DOI: 10.1097/MMR.0b013e3283587727. URL: <http://content.wkhealth.com/linkback/openurl?sid=WKPTLP:landingpage&an=00013542-201301000-00002> (visited on 04/09/2019).
- [20] Jed F. Fisher, Samy O. Meroueh, and Shahriar Mobashery. “Bacterial Resistance to beta-Lactam Antibiotics: Compelling Opportunism, Compelling Opportunity”. In: *Chemical Reviews* 105.2 (Feb. 1, 2005), pp. 395–424. ISSN: 0009-2665. DOI: 10.1021/cr030102i. URL: <https://doi.org/10.1021/cr030102i> (visited on 04/09/2019).
- [21] Graevemoore. *English: Illustrates differences between Gram-positive and gram-negative bacteria*. Apr. 20, 2008. URL: <https://commons.wikimedia.org/wiki/File:Gram-Cell-wall.svg> (visited on 04/17/2019).

- [22] Sabina Islam, Michael J. Benedik, and Thomas K. Wood. “Orphan Toxin OrtT (YdcX) of Escherichia coli Reduces Growth during the Stringent Response”. In: *Toxins* 7.2 (Jan. 29, 2015), pp. 299–321. ISSN: 2072-6651. DOI: 10.3390/toxins7020299. URL: <https://www.ncbi.nlm.nih.gov/pmc/articles/PMC4344625/> (visited on 05/02/2019).
- [23] Anne de Jong et al. “PePPER: a webserver for prediction of prokaryote promoter elements and regulons”. In: *BMC Geno-s* (2011).
- [24] Eili Y. Klein et al. “Global increase and geographic convergence in antibiotic consumption between 2000 and 2015”. In: *Proceedings of the National Academy of Sciences* 115.15 (Apr. 10, 2018), E3463–E3470. ISSN: 0027-8424, 1091-6490. DOI: 10.1073/pnas.1717295115. URL: <https://www.pnas.org/content/115/15/E3463> (visited on 06/13/2019).
- [25] N. C. Klein and B. A. Cunha. “Third-generation cephalosporins”. In: *The Medical Clinics of North America* 79.4 (July 1995), pp. 705–719. ISSN: 0025-7125.
- [26] Sergey Koren et al. “Canu: scalable and accurate long-read assembly via adaptive k-mer weighting and repeat separation”. In: *Genome Research* 27.5 (May 1, 2017), pp. 722–736. ISSN: 1088-9051, 1549-5469. DOI: 10.1101/gr.215087.116. URL: <http://genome.cshlp.org/content/27/5/722> (visited on 04/30/2019).
- [27] Alexandre P. Kuzin et al. “Structure of the SHV-1 β -Lactamase”. In: *Biochemistry* 38.18 (May 1, 1999), pp. 5720–5727. ISSN: 0006-2960. DOI: 10.1021/bi990136d. URL: <https://doi.org/10.1021/bi990136d> (visited on 04/10/2019).
- [28] R. Leclercq et al. “EUCAST expert rules in antimicrobial susceptibility testing”. In: *Clinical Microbiology and Infection: The Official Publication of the European Society of Clinical Microbiology and Infectious Diseases* 19.2 (Feb. 2013), pp. 141–160. ISSN: 1469-0691. DOI: 10.1111/j.1469-0691.2011.03703.x.
- [29] Heng Li and Richard Durbin. “Fast and accurate short read alignment with Burrows-Wheeler transform”. In: *Bioinformatics (Oxford, England)* 25.14 (July 15, 2009), pp. 1754–1760. ISSN: 1367-4811. DOI: 10.1093/bioinformatics/btp324.
- [30] *Modelling the antibiotic development process*. URL: <https://amr-review.org/sites/default/files/Modelling%20the%20antibiotic%20development%20process.pdf> (visited on 04/17/2019).
- [31] *mp6 Piezoelectric Diaphragm Micropump*. URL: <https://www.servoflo.com/micropumps/mp6> (visited on 04/16/2019).
- [32] Jose M. Munita and Cesar A. Arias. “Mechanisms of Antibiotic Resistance”. In: *Microbiology spectrum* 4.2 (Apr. 2016). ISSN: 2165-0497. DOI: 10.1128/microbiolspec.VMBF-0016-2015. URL: <https://www.ncbi.nlm.nih.gov/pmc/articles/PMC4888801/> (visited on 04/11/2019).

- [33] Sergey Nurk et al. “Assembling single-cell genomes and mini-metagenomes from chimeric MDA products”. In: *Journal of Computational Biology: A Journal of Computational Molecular Cell Biology* 20.10 (Oct. 2013), pp. 714–737. ISSN: 1557-8666. DOI: 10.1089/cmb.2013.0084.
- [34] Stephen R. Palumbi. “Humans as the World’s Greatest Evolutionary Force”. In: *Science* 293.5536 (Sept. 7, 2001), pp. 1786–1790. ISSN: 0036-8075, 1095-9203. DOI: 10.1126/science.293.5536.1786. URL: <https://science.sciencemag.org/content/293/5536/1786> (visited on 04/11/2019).
- [35] Franziska Pfeiffer et al. “Systematic evaluation of error rates and causes in short samples in next-generation sequencing”. In: *Scientific Reports* 8.1 (July 19, 2018), p. 10950. ISSN: 2045-2322. DOI: 10.1038/s41598-018-29325-6. URL: <https://www.nature.com/articles/s41598-018-29325-6> (visited on 04/15/2019).
- [36] *Pilon: An Integrated Tool for Comprehensive Microbial Variant Detection and Genome Assembly Improvement*. URL: <https://journals.plos.org/plosone/article?id=10.1371/journal.pone.0112963> (visited on 04/30/2019).
- [37] *Resolving structural diversity of Carbapenemase-producing gram-negative bacteria using single molecule sequencing — bioRxiv*. URL: <https://www.biorxiv.org/content/10.1101/456897v1> (visited on 04/15/2019).
- [38] Torsten Seemann. *:zap: :aquarius: Rapid prokaryotic genome annotation: tseemann/prokka*. original-date: 2014-03-26T07:19:23Z. Apr. 11, 2019. URL: <https://github.com/tseemann/prokka> (visited on 04/15/2019).
- [39] Torsten Seemann. “Prokka: rapid prokaryotic genome annotation”. In: *Bioinformatics (Oxford, England)* 30.14 (July 15, 2014), pp. 2068–2069. ISSN: 1367-4811. DOI: 10.1093/bioinformatics/btu153.
- [40] *SmartTable All promoters of E. coli K-12 substr. MG1655*. URL: <https://biocyc.org/group?id=ALL-PROMOTERS&orgid=ECOLI> (visited on 06/14/2019).
- [41] *SmartTable: All promoters of E. coli K-12 substr. MG1655*. Apr. 2, 2019. URL: <https://www.bag.admin.ch/bag/de/home/krankheiten/infektionskrankheiten-bekaempfen/antibiotikaresistenzen/wie-viele-antibiotika-verbrauchen-wir---.html>.
- [42] Ivan Sović et al. “Fast and sensitive mapping of nanopore sequencing reads with GraphMap”. In: *Nature Communications* 7 (Apr. 15, 2016), p. 11307. ISSN: 2041-1723. DOI: 10.1038/ncomms11307. URL: <https://www.nature.com/articles/ncomms11307> (visited on 04/16/2019).
- [43] F Tissot et al. “Enterobacteriaceae mit Breitspektrum Beta-Laktamasen (ESBL) im Spital: Neue Empfehlungen Swissnoso 2014”. In: 2 (), p. 8.
- [44] Erdal Toprak et al. “Building a morbidostat: an automated continuous-culture device for studying bacterial drug resistance under dynamically sustained drug inhibition”. In: *Nature Protocols* 8.3 (Mar. 2013), pp. 555–567. ISSN: 1750-2799. DOI: 10.1038/nprot.nprot.2013.021.
- [45] C. Lee Ventola. “The Antibiotic Resistance Crisis”. In: *Pharmacy and Therapeutics* (2015).

- [46] C. Lee Ventola. “The Antibiotic Resistance Crisis”. In: *Pharmacy and Therapeutics* 40.4 (Apr. 2015), pp. 277–283. ISSN: 1052-1372. URL: <https://www.ncbi.nlm.nih.gov/pmc/articles/PMC4378521/> (visited on 04/11/2019).
- [47] Ryan R. Wick et al. “Unicycler: Resolving bacterial genome assemblies from short and long sequencing reads”. In: *PLOS Computational Biology* 13.6 (June 8, 2017), e1005595. ISSN: 1553-7358. DOI: 10.1371/journal.pcbi.1005595. URL: <https://journals.plos.org/ploscompbiol/article?id=10.1371/journal.pcbi.1005595> (visited on 04/15/2019).
- [48] Gerard D. Wright. *English: Antibiotic targets and mechanisms of resistance*. 2010. URL: https://commons.wikimedia.org/wiki/File:Antibiotic_resistance_mechanisms.jpg (visited on 06/13/2019).

Chapter 9

Acknowledgements

inputasdfasdfsdafsaf